



Università degli Studi di Napoli Federico II

Scuola Politecnica e delle Scienze di Base
Corso di Laurea in Ingegneria Aerospaziale

TESI DI LAUREA
IN
INGEGNERIA AEROSPAZIALE

**Assessment of complete aircraft
lateral-directional stability and control characteristics
using JPAD (Java toolchain of Programs for Aircraft Design)**

Relatore:

Prof. Ing. Agostino De Marco

Correlatore:

Ing. Manuela Ruocco

Candidato:

Carmine Vaselli

Matricola N35/1920

*Ever tried. Ever failed. No matter.
Try again. Fail again. Fail better.*
– Samuel Beckett

ABSTRACT

This thesis project involves developing some modules of the java library named JPAD, which stands for Java toolchain of Programs for Aircraft Design. These modules refer to conventional airplanes flying at subsonic speeds and have been set up to compute aerodynamic coefficients, with regard to lateral-directional motion. The calculation formulas are mostly based on the book by Napolitano [9] and USAF DATCOM [7].

Firstly in this work it is introduced the structure of JPAD library. Then the empirical methods and the formulas used in the processing functions are presented. Next a numerical test made on a regional turboprop is shown. And finally, in an appendix, it is presented how charts digitization has been made.

SOMMARIO

Questo progetto di tesi prevede lo sviluppo di alcuni moduli della libreria java denominata JPAD (Java toolchain di Programs for Aircraft Design). Questi moduli si riferiscono ad aeroplani convenzionali che volano a velocità subsoniche e sono stati creati per calcolare i coefficienti aerodinamici relativi al moto latero-direzionale. Le formule di calcolo sono per lo più basate sul libro di Napolitano [9] e USAF DATCOM [7].

In primo luogo in questo scritto sarà introdotta la struttura della libreria JPAD. Quindi saranno presentati i metodi empirici e le formule utilizzate nelle funzioni di calcolo. Successivamente sarà effettuato un test numerico su un turboelica regionale. E infine, in un'appendice, viene presentato il modo con cui è stata realizzata la digitalizzazione dei grafici.

Contents

1	Introduction to JPAD	1
1.1	Software structure	1
1.2	The Java Language	5
1.3	Java choice	5
2	Calculation formulas	7
2.1	Steady-state lateral force coefficient	7
2.1.1	Sideslip angle effect	7
2.1.2	Ailerons deflection effect	9
2.1.3	Rudder deflection effect	9
2.2	Steady-state rolling moment coefficient	11
2.2.1	Dihedral effect	11
2.2.2	Ailerons deflection effect	12
2.2.3	Rudder deflection effect	20
2.3	Steady-state yawing moment coefficient	20
2.3.1	Weathercock effect	21
2.3.2	Ailerons deflection effect	22
2.3.3	Rudder deflection effect	22
2.4	Unsteady-state lateral force coefficient	24
2.4.1	Roll rate effect	24
2.4.2	Yaw rate effect	24
2.5	Unsteady-state rolling moment coefficient	24
2.5.1	Roll rate effect	24
2.5.2	Yaw rate effect	26
2.6	Unsteady-state yawing moment coefficient	28
2.6.1	Roll rate effect	28
2.6.2	Yaw rate effect	29
3	Example of application on a regional turboprop	32
A	HDF dataset and database reader creation	36
A.1	Chart digitization	36
A.2	Creation of an HDF file with MATLAB	37
	List of symbols	41
	Bibliography	43

Introduction to JPAD

Nowadays the preliminary design phase of an aircraft is becoming very challenging due to the need for more demanding requirements which deals with different fields of applications. In this perspective, there is a certain need for simple design tools both in aircraft industries and academic research groups which can perform fast and reliable multi-disciplinary analyses and optimizations.

This chapter provides a comprehensive overview of JPAD (Java toolchain of Programs for Aircraft Design) [4], a Java-based open-source library conceived as a fast and efficient tool useful as support in the preliminary design phases of an aircraft, and during its optimization process. The library has been completely realized at the Department of Industrial Engineering of the University of Naples “Federico II” where is still in development.

One of the main features of JPAD lies in the smart management of both the aircraft parametric model, which is conceived as a set of interconnected and parameterized components, and the available analyses. The library has been developed with the purpose of simplify the composition of the input file for the user and doing fast analysis with a satisfying grade of accuracy. The following section will focus on the description of the software structure and its main advantages. Another key point is the possibility to easily interface JPAD with other external tools in order to achieve a higher level of accuracy.

The JPAD library is an alternative to a plethora of similar software tools, both freeware and commercial [3] [8] [11]. Most of these tools have an important history, and many of them have been in use for decades. Some of them were conceived with poor software design criteria, have a rigid textual input and come with no visualization features. This is the main reason why JPAD has been developed paying a lot of attention to simplicity and flexibility. Moreover, it has been conceived as an open-source tool.

1.1 Software structure

To achieve a clear input file organization a considerable study has been done. The result is an input structure composed by different XML files with the purpose to allow users to easily manage all data needed to execute the desired analyses. In figure 1.1 on the following page the entire structure of the software is schematized. It is possible to clearly note that there are two main blocks: input and core.

The input block is defined by two main parts: aircraft and analyses definitions. The first one defines the aircraft model in parametric way using a main file (Aircraft.xml, see figure 1.3) which collects all the components, linking them to their related XML file (i.e.

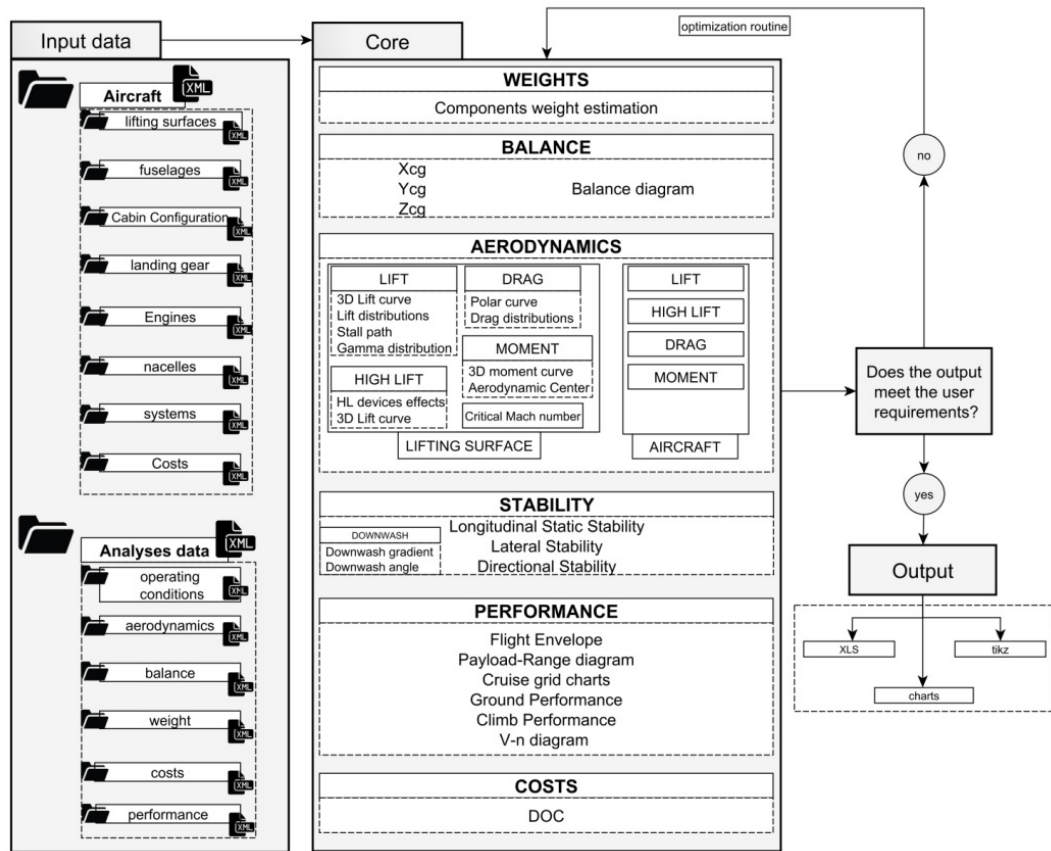


Figure 1.1. JPAD schematic flow-chart

```

1  <?xml version="1.0" encoding="utf-8"?>
2  <jpad_config>
3      <!-- Input data, shared across analysis tasks -->
4      <global_data>
5          <n_limit>2.5</n_limit>
6          <cruise_lift_coefficient>0.45</cruise_lift_coefficient>
7          <reference_range unit="nmi">825</reference_range>
8          <maximum_altitude_at_maximum_speed unit="ft">16000</
9              maximum_altitude_at_maximum_speed>
10         <maximum_cruise_mach_number>0.43</
11             maximum_cruise_mach_number>
12         <optimum_cruise_altitude unit="ft">16000</
13             optimum_cruise_altitude>
14         <optimum_cruise_mach_number>0.45</
15             optimum_cruise_mach_number>
16         <block_time unit="h">1.5</block_time>
17         <flight_time unit="h">1.35</flight_time>
18     </global_data>
19     <!-- Required analysis tasks -->
20     <analyses id="JPAD Test analysis">
21         <weights>
22             file="analysis_weights.xml"
23             method_fuselage="JENKINSON"
24             method_wing="ROSKAM"
25             method_htail="JENKINSON"
26             method_vtail="JENKINSON"
27             method_canard=""
28             method_nacelles="TORENBEEK_1976"
29             method_landing_gears="ROSKAM"
30             method_systems="TORENBEEK_2013"
31             <!-- method_XXX="AVERAGED" if not present -->
32         </weights>
33         <balance>
34             file="analysis_balance.xml"
35             method_fuselage=""
36             method_wing=""
37             method_htail=""
38             method_vtail=""
39             method_canard=""
40             <!-- method_XXX="AVERAGED" if not present -->
41         </balance>
42         <aerodynamics file="analysis_aerodynamics.xml"/>
43         <performance file="analysis_performance.xml"/>
44         <costs file="analysis_costs.xml"/>
45     </analyses>
46 </jpad_config>

```

Figure 1.2. An example of the analysis.xml file



Figure 1.3. An extract from a general Aircraft.xml input file

fuselage.xml, vtail.xml, and so on) which contains all geometrical data.

The second one defines all necessary data for each analysis presents into core module (see figure 1.2). Since the aircraft model contains only geometrical data, it is necessary to define several further data referred to each analysis.

The structure described above allows to generate different aircrafts, or different configurations of the same model, combining different components. The possibility to generate a series of different aircrafts in a simple and fast way, allows to easily perform comparisons between these latter. For example, assuming different wings and engines, it is possible to estimate the effects that some design parameters have on a specific output. Figure 1.4 shows how the FAR-25 take-off field length behaves with different values of the wing surface and the engine static thrust at fixed aircraft maximum take-off weight. This feature plays also a key role in the optimization process described in figure 1.1.

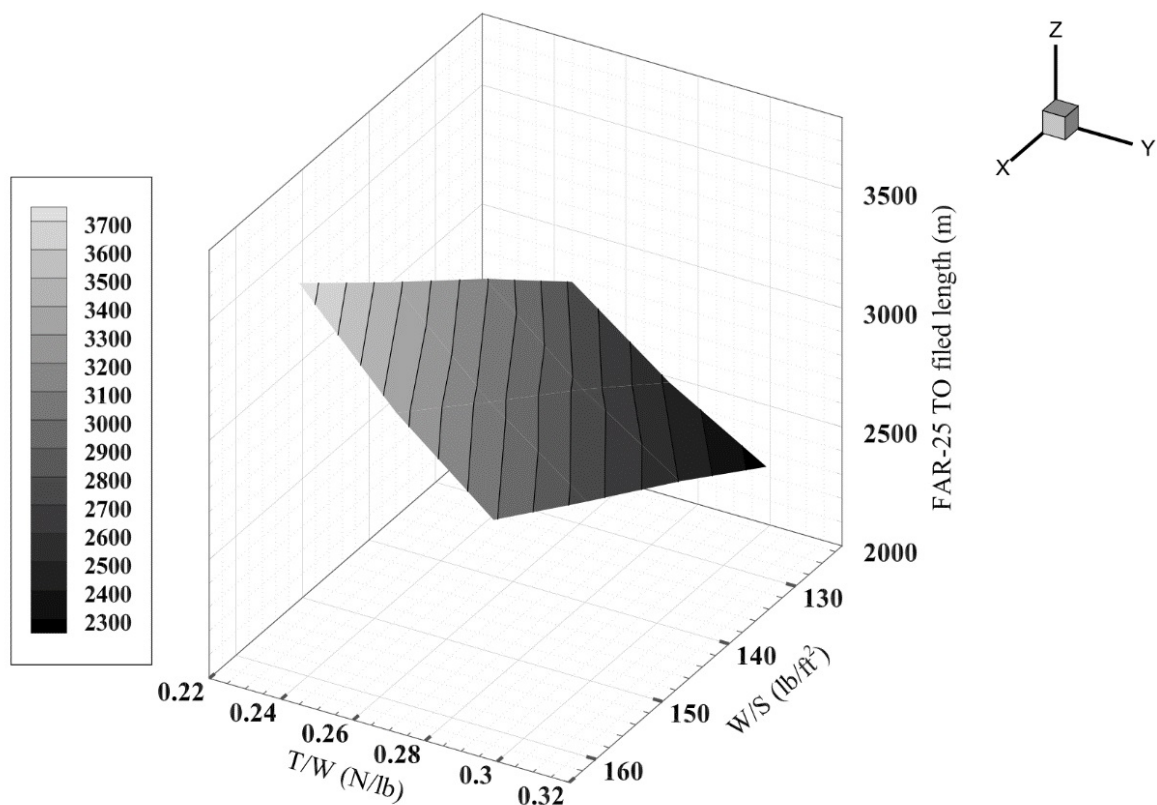


Figure 1.4. FAR-25 take-off field length at different wing loadings and thrust-weight ratios

In the same way, it is possible to perform a complete analysis (those present into core block in figure 1.1), or a specific one, combining different analyses files. This allows an easier evaluation of generic cost function during optimization tasks, resulting in reduced amount of computational costs required for this kind of operations.

Besides the input, the second main block is the core, which manages all the available analyses. This contains several independent modules, as shown in the figure 1.1, that deals with following application fields.

- **Weights:** estimates the aircraft weight breakdown starting from a first guess maximum take-off weight and some mission requirements. In particular, it evaluates each aircraft component mass using well-known semi-empirical equations.
- **Balance:** estimates the centre of gravity position related to each weight condition and draws the balance diagram.

- **Aerodynamics and Stability:** the aerodynamics module estimates all the aerodynamic characteristics concerning lift, drag and moments coefficients at different operating conditions for each aircraft component (wing, tails, fuselage and nacelles), whereas the stability module gives useful data about static stability of the whole aircraft.
- **Performance:** evaluates most important aircraft performance such as Payload-Range diagram, mission profile, cruise flight envelope, ground performance, climb performance and the cruise grid chart.
- **Costs:** estimates the DOC (Direct Operating Costs) breakdown.

Finally, JPAD allows to obtain different kind of output: charts and data in XLS format.

1.2 The Java Language

Java was developed by Sun Microsystems, a company that was incorporated in Oracle from a few years. This programming language is a general-purpose, concurrent, class-based, object-oriented language. It is designed to be simple enough that many programmers can achieve fluency in the language [5].

One design goal of Java is portability, which means that programs written for the Java platform must run similarly on any combination of hardware and operating system with adequate runtime support. This is achieved by compiling the Java language code to an intermediate representation called Java bytecode, instead of directly to architecture-specific machine code. Java bytecode instructions are analogous to machine code, but they are intended to be executed by a virtual machine (VM) written specifically for the host hardware. End users commonly use a Java Runtime Environment (JRE) installed on their own machine for standalone Java applications, or in a web browser for Java applets [2].

There were five primary goals in the creation of the Java language [10]:

- it must be “simple, object-oriented, and familiar”;
- it must be “robust and secure”;
- it must be “architecture-neutral and portable”;
- it must execute with “high performance”;
- it must be “interpreted, threaded, and dynamic”.

Actually Java is the most used programming language according to TIOBE (see figure 1.5 on the following page). The TIOBE Programming Community index is an indicator of the popularity of programming languages. The ratings are based on the number of skilled engineers world-wide, courses and third party vendors.

1.3 Java choice

The choice of Java as the programming language was driven by several considerations. These include the following:

- the language should be widely supported; this to avoid the case of many valid aircraft design applications and libraries that became obsolete due to the aging of the programming language used to build them;

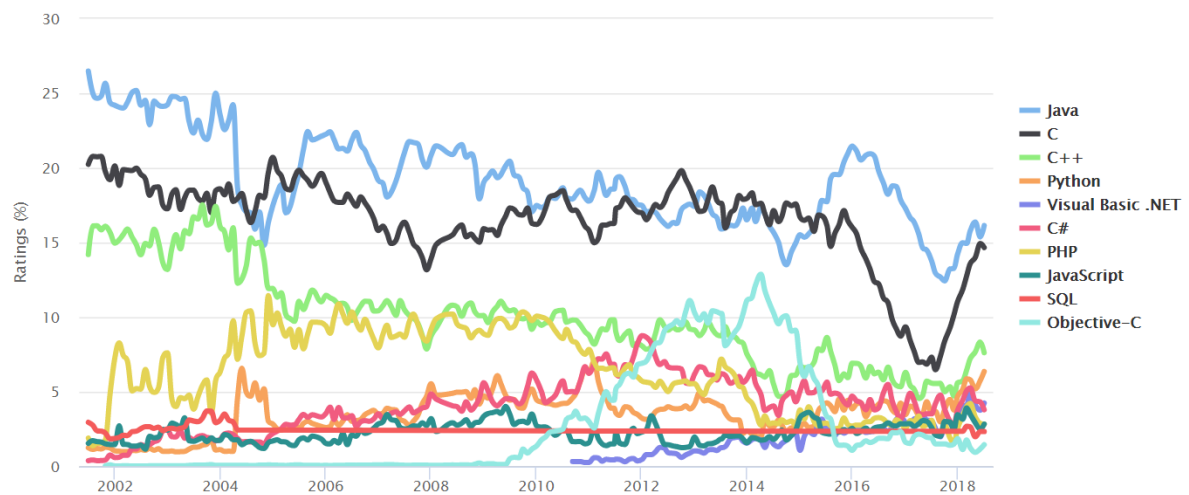


Figure 1.5. TIOBE Programming Community index (www.tiobe.com)

- the language is object oriented;
- the language should promote the use of open source libraries, especially for I/O tasks and for complex mathematical operations;
- the language and the companion Integrated Development Environment (IDE) should provide a widely supported Graphical User Interface (GUI) framework and a GUI visual builder;
- the language should support and promote modularity.

The Java programming language meets all these requirements; moreover it is backed by Oracle and by a huge community of developers so it is continuously updated. Also, advanced and free IDEs (such as Eclipse) allow programmers to streamline and simplify the development process; in particular, the Eclipse IDE has been chosen to develop JPAD.

Being Java a pure object oriented programming language, it greatly encourages and simplifies modularization. Each module (package) can be programmed quite independently so that it is relatively easy to divide the work among several programmers. This is essential since the amount of classes and calculations needed to abstract, manage and analyse the entire aircraft is very large (presently the whole project counts more than 10 millions lines of code). For such a reason the establishment of common practices and the adherence to fundamental principle of software development (*Don't Repeat Yourself*, *Separation of Concerns*, *Agile software development*) are equally important.

Calculation formulas

The purpose of this chapter is to provide the calculation formulas implemented in JPAD software and used to evaluate the aerodynamic coefficients with regard to the aircraft as a whole. The calculation formulas are mostly based on the well known USAF DATCOM [7]. In particular, both for the specific formulations and for the symbols, we have used a single reference, namely the textbook by Napolitano [9].

In the following we will recall some of the most important formulas used to model the lateral force coefficient and the rolling and yawing moment coefficients. These assume the validity of the superposition principle and express all quantities referred to the aircraft as a sum of a number of contributions. Each aerodynamic coefficient is computed first evaluating the contribution due to each part taken singularly; then the extra contribution due to aerodynamic interferences are estimated; finally, all contributions are summed up.

From now on, all the angular gradients will be evaluated in rad^{-1} .

2.1 Steady-state lateral force coefficient

The steady-state lateral force can be evaluated by the relationship:

$$Y = C_Y \bar{q} S_W \quad (2.1)$$

where the lateral force coefficient can be expressed by:

$$C_Y = f(\beta, \delta_a, \delta_r) \quad (2.2)$$

The first order approximation for the Taylor expansion gives the following expression for C_Y :

$$C_Y = C_{Y_0} + C_{Y_\beta} \beta + C_{Y_{\delta_a}} \delta_a + C_{Y_{\delta_r}} \delta_r \quad (2.3)$$

in which the term C_{Y_0} is zero if the aircraft is symmetric with respect to the XZ plane.

2.1.1 Sideslip angle effect

The aerodynamic coefficient C_{Y_β} can be expressed through its dependencies as shown in the following formula:

$$C_{Y_\beta} = C_{Y_{\beta, \text{WB}}} + C_{Y_{\beta, \text{H}}} + C_{Y_{\beta, \text{V}}} \quad (2.4)$$

In this equation there are the contributions of the wing-body configuration, of the horizontal tail and of the vertical tail. For a detailed modelling of C_{Y_β} , it is useful to separate the contribution of the wing and of the fuselage:

$$C_{Y_\beta} = C_{Y_{\beta,W}} + C_{Y_{\beta,B}} + C_{Y_{\beta,H}} + C_{Y_{\beta,V}} \quad (2.5)$$

A relationship for the wing contribution is given by:

$$C_{Y_{\beta,W}} = -0.00573|\Gamma_W| \quad (2.6)$$

A relationship for the fuselage contribution is instead given by:

$$C_{Y_{\beta,B}} = -2K_{\text{int}} \frac{S_{P \rightarrow V}}{S_W} \quad (2.7)$$

where k_{int} is an interference factor calculated from figure 2.1, whereas $S_{P \rightarrow V}$ is the cross section at the location of the fuselage where the flow ceases to be potential.

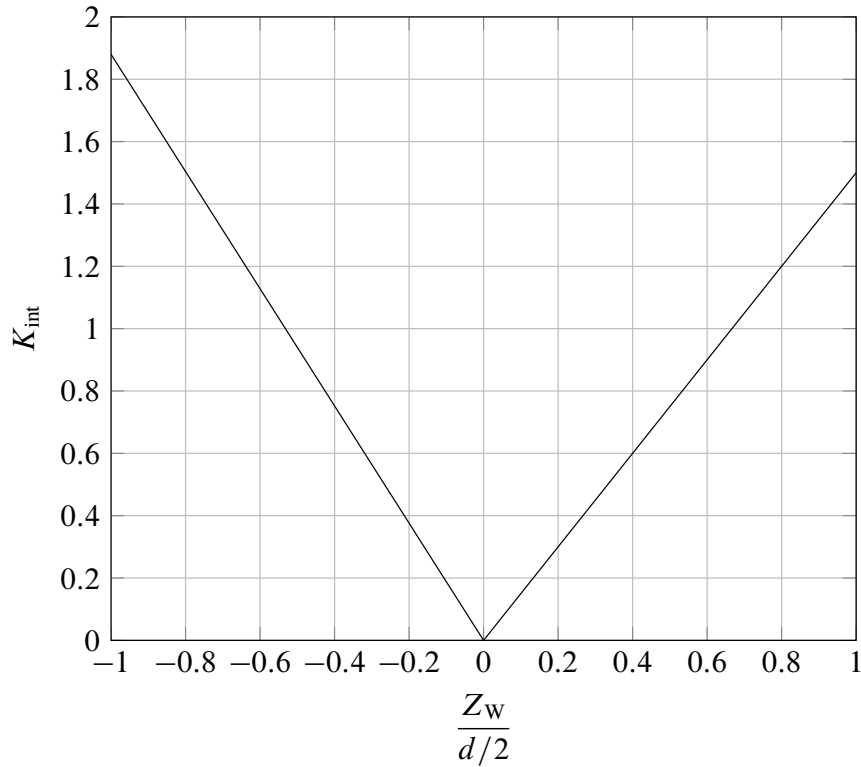


Figure 2.1. Wing-body interference factor

The horizontal tail contribution is given by:

$$C_{Y_{\beta,H}} = -0.00573|\Gamma_H|\eta_H \left(1 - \frac{d\sigma}{d\beta}\right) \frac{S_H}{S_W} \quad (2.8)$$

The vertical tail contribution is expressed in the following formula:

$$C_{Y_{\beta,V}} = -k_{Y_V}|C_{L_{\alpha,V}}|\eta_V \left(1 - \frac{d\sigma}{d\beta}\right) \frac{S_V}{S_W} \quad (2.9)$$

where k_{Y_V} is an empirical factor shown in figure 2.2 on the following page.

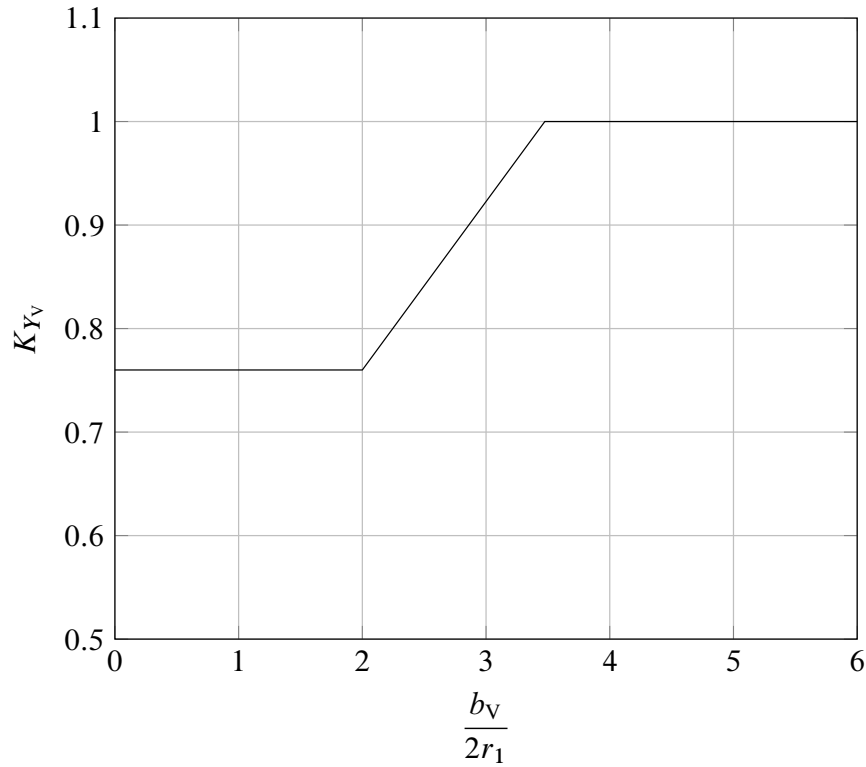


Figure 2.2. Empirical factor for the lateral force at the vertical tail due to β

2.1.2 Ailerons deflection effect

The ailerons are an asymmetric control surface and the forces associated with their deflections act along the vertical and horizontal directions; therefore, their components along the lateral direction is negligible. Thus, we have:

$$C_{Y_{\delta_a}} \approx 0 \quad (2.10)$$

2.1.3 Rudder deflection effect

The rudder is a control surface. A mathematical relationship for $C_{Y_{\delta_r}}$ is given by:

$$C_{Y_{\delta_r}} = |C_{L_{\alpha_v}}| \eta_v \frac{S_v}{S_w} \Delta(K_r) \tau_r \quad (2.11)$$

In this relationship the term $C_{L_{\alpha_v}}$ is the lift-curve slope for the vertical tail, $\Delta(K_r)$ is a correction factor associated with the span of the rudder within the span of the vertical tail, evaluated graphically from figure 2.3 on the next page using η of the inner and outer rudder station, and τ_r is a control surface effectiveness factor, calculated from figure 2.4 on the following page.

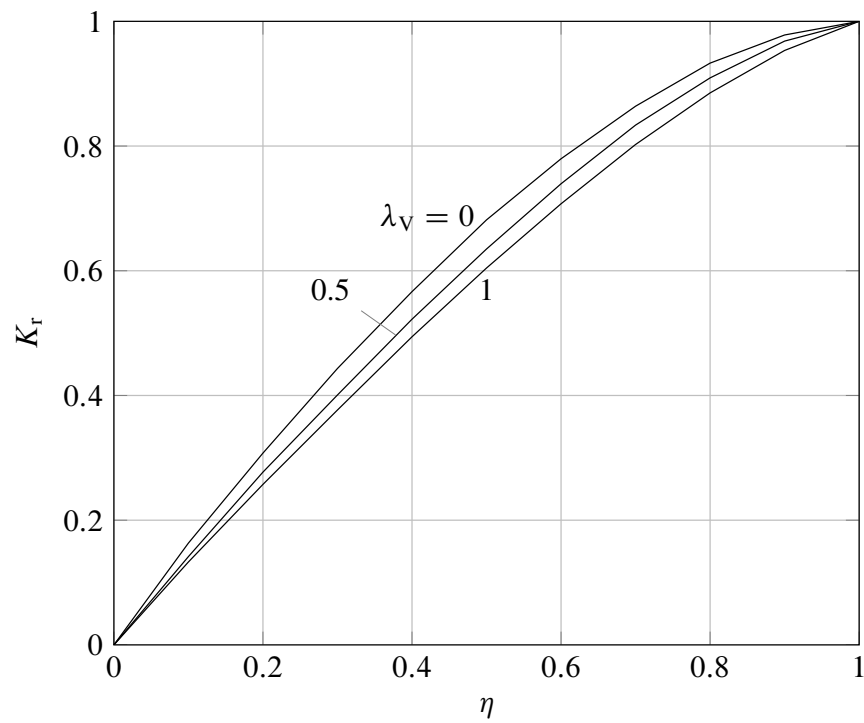


Figure 2.3. Span factor between rudder and vertical tail

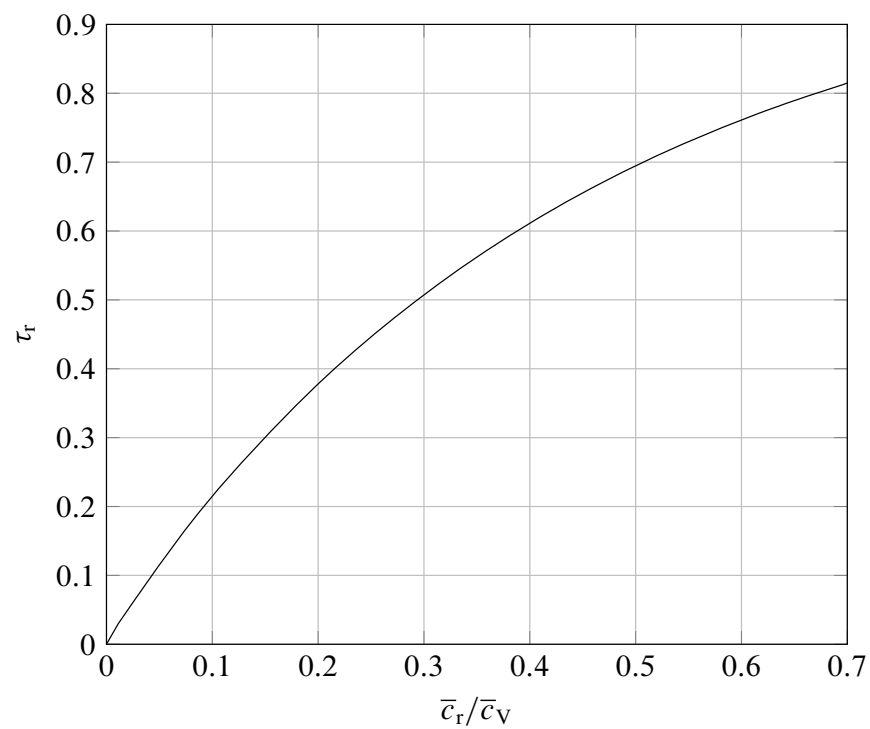


Figure 2.4. Effectiveness of the rudder τ_r as function of \bar{c}_r/\bar{c}_v

2.2 Steady-state rolling moment coefficient

The steady-state rolling moment can be evaluated by the relationship:

$$\mathcal{L} = C_{\mathcal{L}} \bar{q} S_W b_W \quad (2.12)$$

where the rolling moment coefficient can be expressed by:

$$C_{\mathcal{L}} = f(\beta, \delta_a, \delta_r) \quad (2.13)$$

The first order approximation for the Taylor expansion gives the following expression for $C_{\mathcal{L}}$:

$$C_{\mathcal{L}} = C_{\mathcal{L}_0} + C_{\mathcal{L}_\beta} \beta + C_{\mathcal{L}_{\delta_a}} \delta_a + C_{\mathcal{L}_{\delta_r}} \delta_r \quad (2.14)$$

in which the term $C_{\mathcal{L}_0}$ is zero if the aircraft is symmetric with respect to the XZ plane.

2.2.1 Dihedral effect

The aerodynamic coefficient $C_{\mathcal{L}_\beta}$ is known as dihedral effect and it can be expressed through its dependencies as shown in the following formula:

$$C_{\mathcal{L}_\beta} = C_{\mathcal{L}_{\beta, WB}} + C_{\mathcal{L}_{\beta, H}} + C_{\mathcal{L}_{\beta, V}} \quad (2.15)$$

In this equation there are the contributions of the wing-body, of the horizontal tail and of the vertical tail.

The contribution of the wing-body consists of three terms: the first one is due to the wing geometric dihedral angle; the second one is due to an aerodynamic phenomenon associated with the location of the fuselage with respect to the wing (high wing or low wing); the third one is due to the geometric wing sweep angle. A closed-form expression for the modelling for $C_{\mathcal{L}_{\beta, WB}}$ is given by:

$$\begin{aligned} C_{\mathcal{L}_{\beta, WB}} = & 57.3 C_L \left[\left(\frac{C_{\mathcal{L}_\beta}}{C_L} \right)_{\Lambda_{c/2}} K_{M_\Lambda} K_f + \left(\frac{C_{\mathcal{L}_\beta}}{C_L} \right)_{AR} \right] + \\ & + 57.3 \left\{ \Gamma_W \left[\frac{C_{\mathcal{L}_\beta}}{\Gamma_W} K_{M_r} + \frac{\Delta C_{\mathcal{L}_\beta}}{\Gamma_W} \right] + (\Delta C_{\mathcal{L}_\beta})_{Z_w} + \varepsilon_W \tan \Lambda_{c/4} \left(\frac{\Delta C_{\mathcal{L}_\beta}}{\varepsilon_W \tan \Lambda_{c/4}} \right) \right\} \end{aligned} \quad (2.16)$$

In the formula 2.16 there are some semi-empirical coefficients:

1. $(C_{\mathcal{L}_\beta}/C_L)_{\Lambda_{c/2}}$ is the contribution associated with the wing sweep angle;
2. K_{M_Λ} is a correction factor associated with the Mach number and the wing sweep angle;
3. K_f is a correction factor associated with the length of the forward portion of the fuselage;
4. $(C_{\mathcal{L}_\beta}/C_L)_{AR}$ is the contribution associated with the wing aspect ratio;
5. $C_{\mathcal{L}_\beta}/\Gamma_W$ is the contribution associated with the wing dihedral angle;
6. K_{M_r} is a correction factor associated with the Mach number and the wing dihedral angle;

7. $\Delta C_{\mathcal{L}_\beta} / \Gamma_W$ is a correction factor associated with the size of the fuselage;
8. $(\Delta C_{\mathcal{L}_\beta})_{Z_W}$ is a correction factor associated with the location of the fuselage with respect to the wing;
9. $\Delta C_{\mathcal{L}_\beta} / (\varepsilon_W \tan \Lambda_{c/4})$ is a correction factor associated with the twist angle ε_W between the zero-lift lines of the wing sections at the tip and at the root stations.

The terms (1), (2), (3), (4), (5), (6) and (9) are given by figure 2.5 on the next page to figure 2.11 on page 16. The term (7) is modelled using the relationship:

$$\frac{\Delta C_{\mathcal{L}_\beta}}{\Gamma_W} = -0.0005 \mathcal{R}_W \left(\frac{d_B}{b_W} \right)^2 \quad (2.17)$$

The factor (8) is modelled using the relationship:

$$(\Delta C_{\mathcal{L}_\beta})_{Z_W} = 1.2 \sqrt{\mathcal{R}_W} \frac{Z_W}{b_W} \left(\frac{2d_B}{b_W} \right) \quad (2.18)$$

The horizontal tail can be considered as a wing, operating at a lower dynamic pressure, with a smaller surface and a smaller span. Therefore, a relationship for $C_{\mathcal{L}_{\beta,H}}$ is given by:

$$C_{\mathcal{L}_{\beta,H}} = C_{\mathcal{L}_{\beta,WB}} \Big|_H \eta_H \frac{S_H}{S_W} \frac{b_H}{b_W} \quad (2.19)$$

where the $C_{\mathcal{L}_{\beta,WB}} \Big|_H$ is the previously introduced $C_{\mathcal{L}_{\beta,WB}}$ evaluated with the geometric parameters of the horizontal tail.

The vertical tail contribution to the dihedral effect is expressed by the following formula:

$$\begin{aligned} C_{\mathcal{L}_{\beta,V}} &= C_{Y_{\beta,V}} \frac{Z_V \cos \alpha_B - X_V \sin \alpha_B}{b_W} = \\ &= -k_{Y_V} |C_{L_{\alpha,V}}| \eta_V \left(1 - \frac{d\sigma}{d\beta} \right) \frac{S_V}{S_W} \frac{Z_V \cos \alpha_B - X_V \sin \alpha_B}{b_W} \end{aligned} \quad (2.20)$$

2.2.2 Ailerons deflection effect

Ailerons are an asymmetric control surface. According to European conventions, a positive deflection of the ailerons implies a trailing edge down deflection of the right aileron and a trailing edge up deflection of the left aileron. The combined result of these deflections is a negative rolling moment. The mathematical expression of $C_{\mathcal{L}_{\delta_a}}$ is:

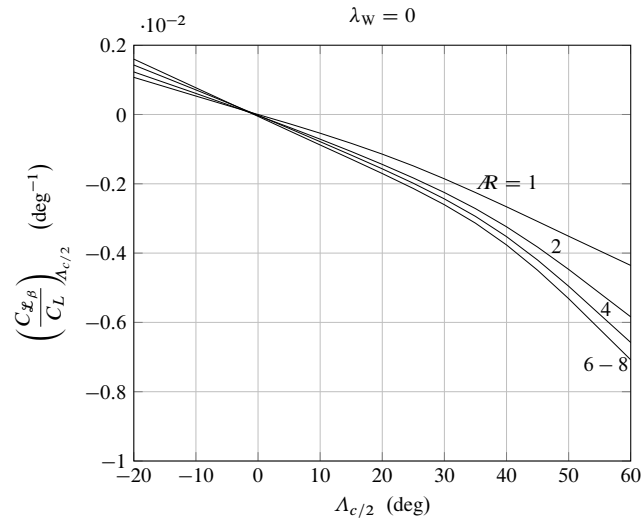
$$C_{\mathcal{L}_{\delta_a}} = C'_{\mathcal{L}_{\delta_a}} \tau_a \quad (2.21)$$

where $C'_{\mathcal{L}_{\delta_a}}$ is given by the following relationship:

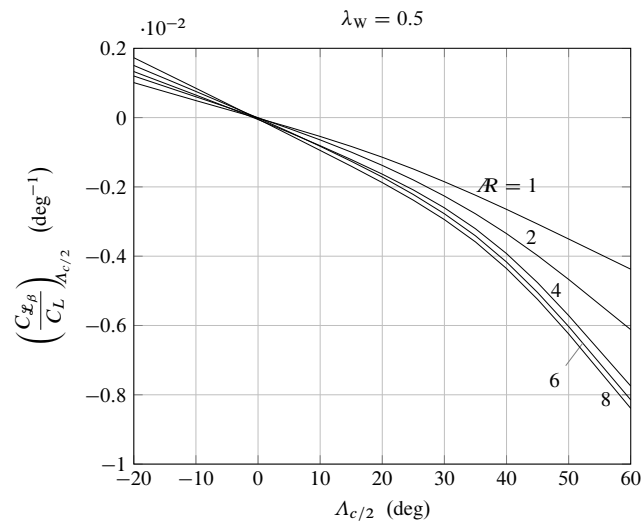
$$C'_{\mathcal{L}_{\delta_a}} = -\Delta(RME) \frac{k}{\sqrt{1-M^2}} \quad (2.22)$$

in which RME is given by charts of figures 2.12 on page 17 to 2.14 on page 19. The term τ_a is a control surface effectiveness factor, calculated from figure 2.15 on page 20. Finally, the term k is equal to:

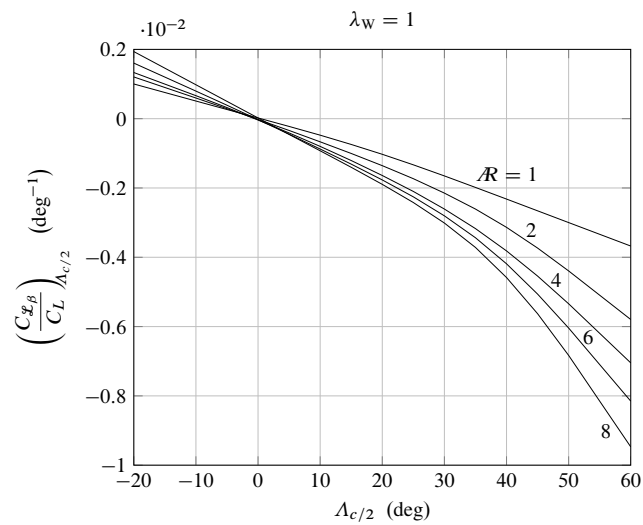
$$k = \frac{C_{L_{\alpha,w}} \sqrt{1-M^2}}{2\pi} \quad (2.23)$$



(a)



(b)



(c)

Figure 2.5. Contribution to $C_{x_{\beta},WB}$ due to wing sweep angle

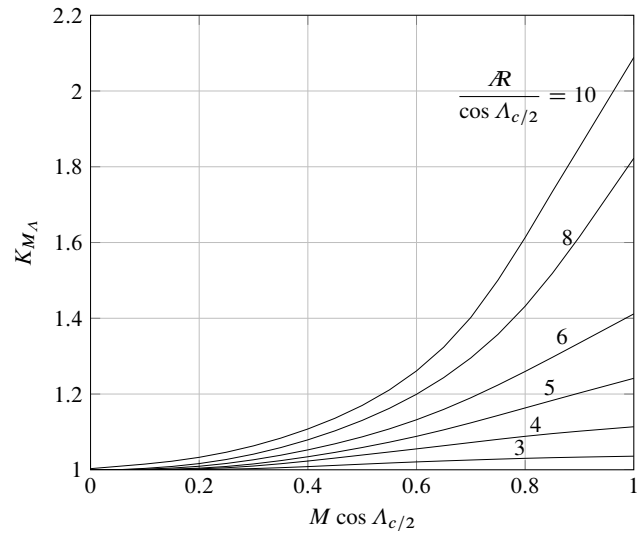


Figure 2.6. Compressibility correction factor for $C_{\mathcal{L}_{\beta, \text{WB}}}$ due to wing sweep angle

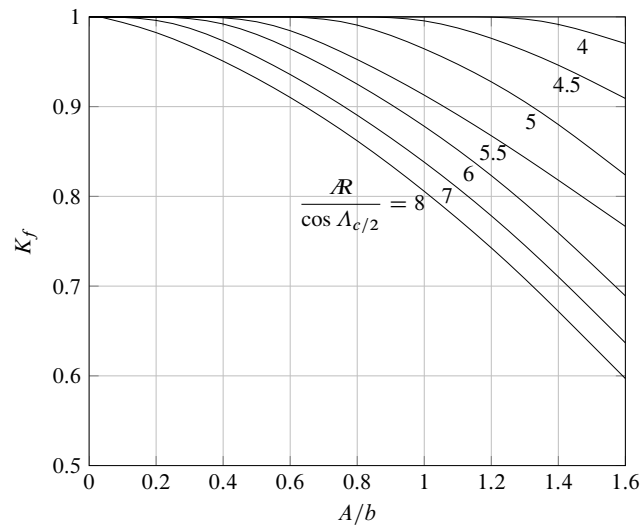


Figure 2.7. Fuselage correction factor for $C_{\mathcal{L}_{\beta, \text{WB}}}$ due to wing sweep angle

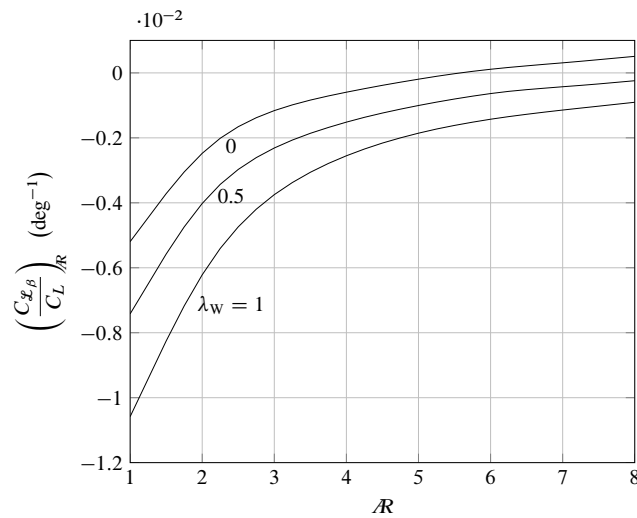


Figure 2.8. Contribution to $C_{\mathcal{L}_{\beta, \text{WB}}}$ due to wing aspect ratio

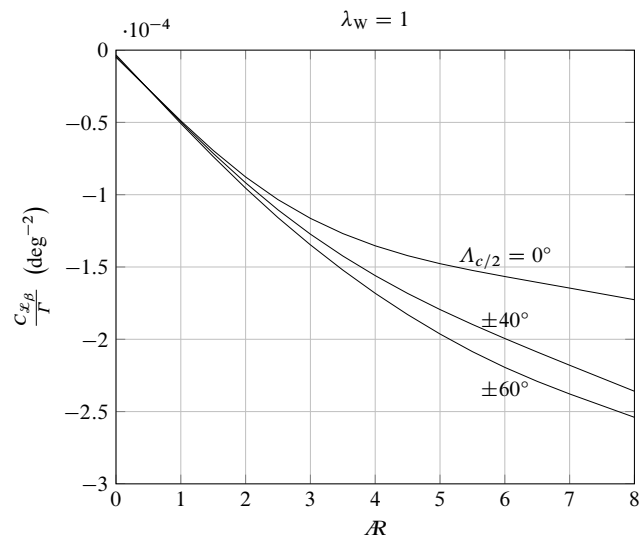
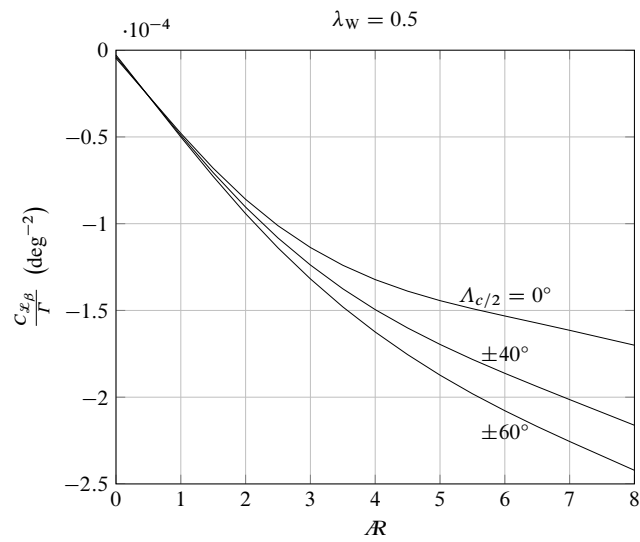
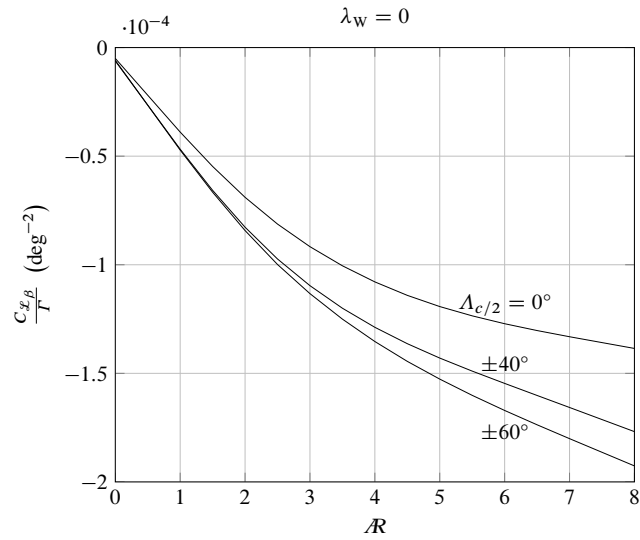


Figure 2.9. Contribution to $C_{x_{\beta, WB}}$ due to wing dihedral angle

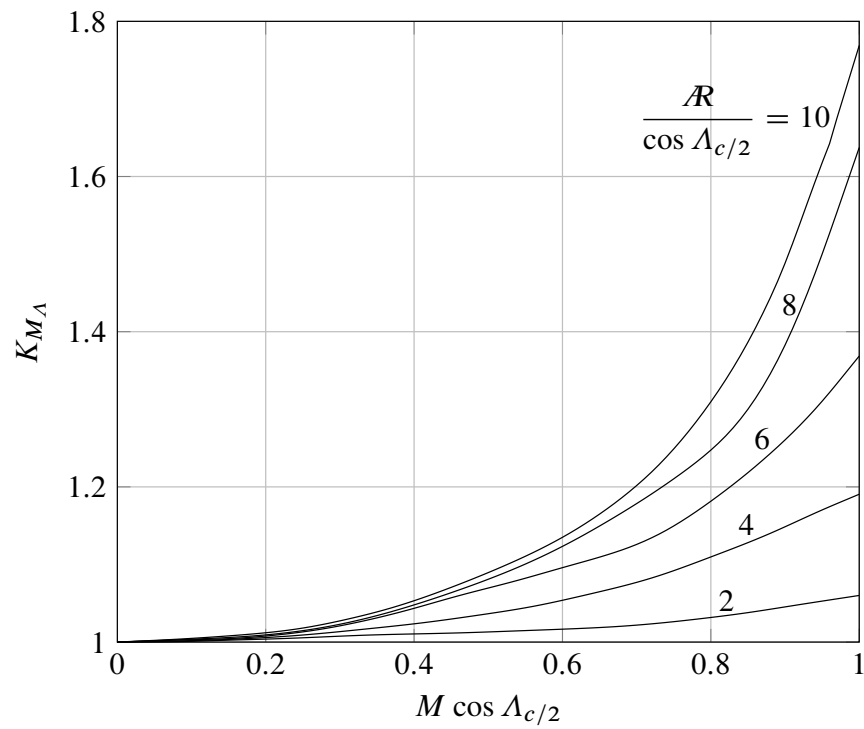


Figure 2.10. Compressibility correction factor for $C_{\mathcal{L}_{\beta, \text{WB}}}$ due to wing dihedral angle

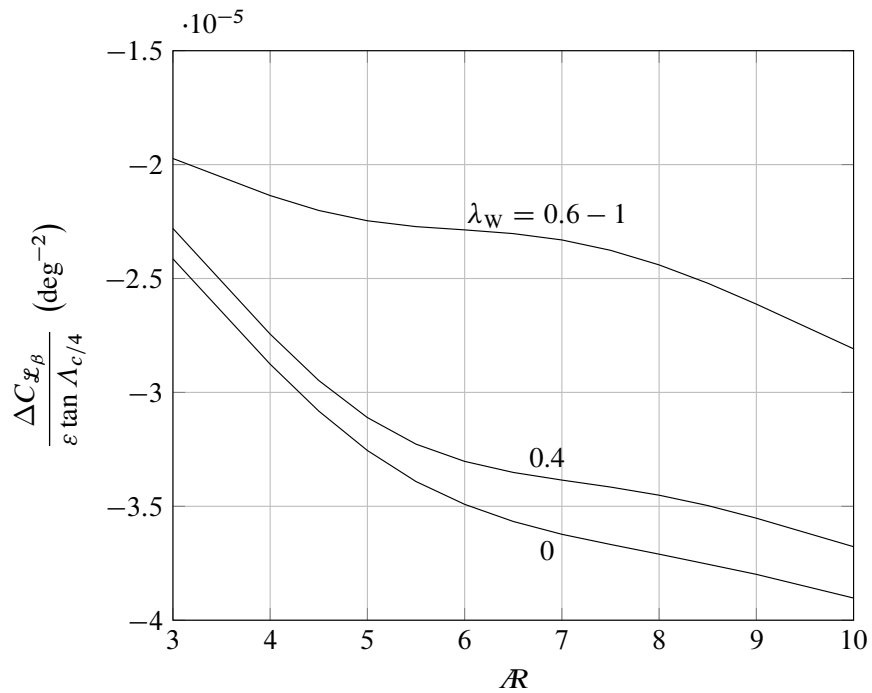
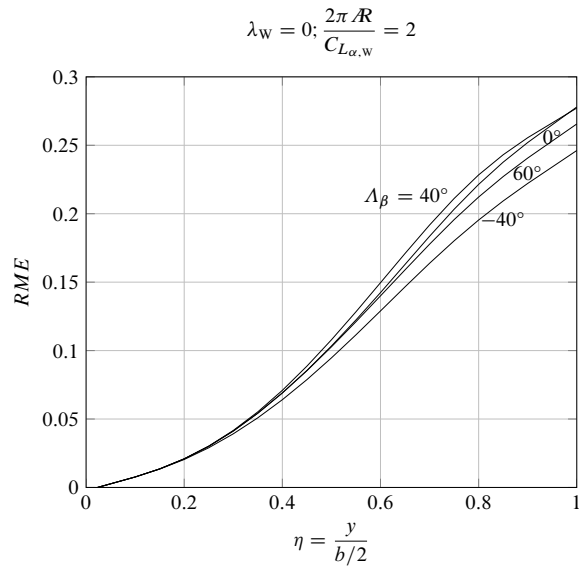
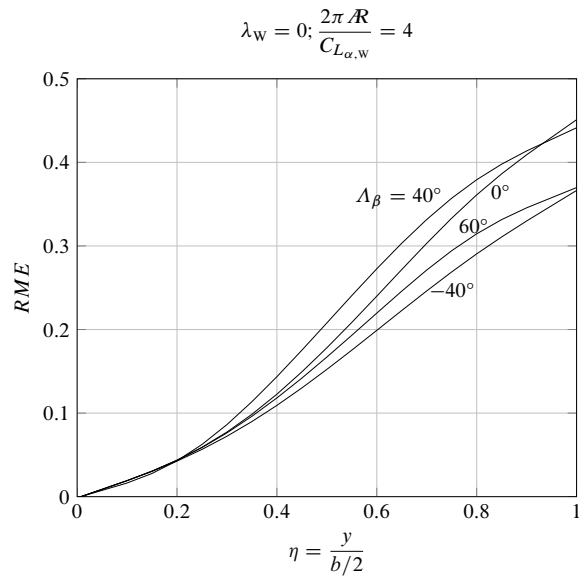


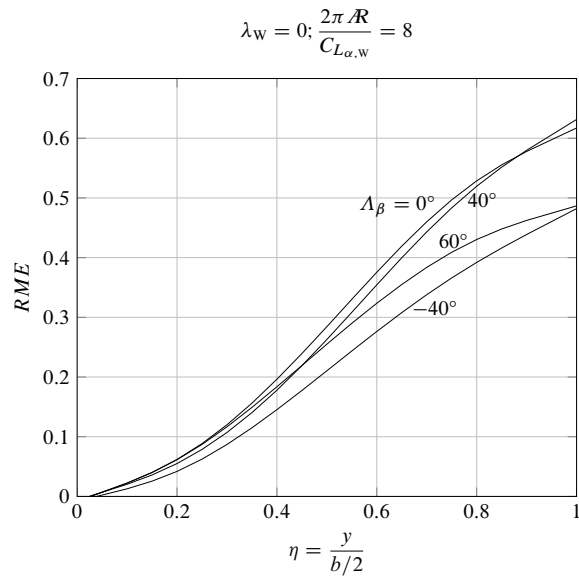
Figure 2.11. Contribution to $C_{\mathcal{L}_{\beta, \text{WB}}}$ due to wing twist angle



(a)

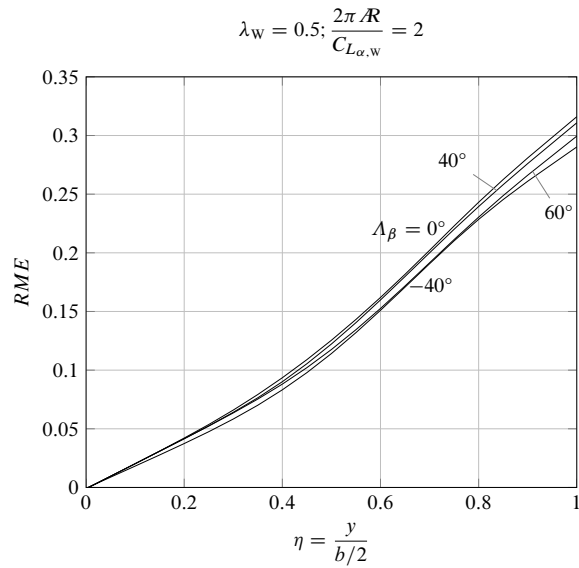


(b)

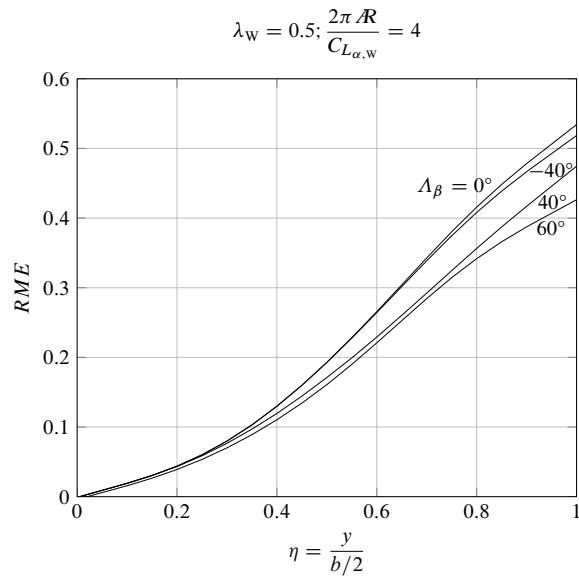


(c)

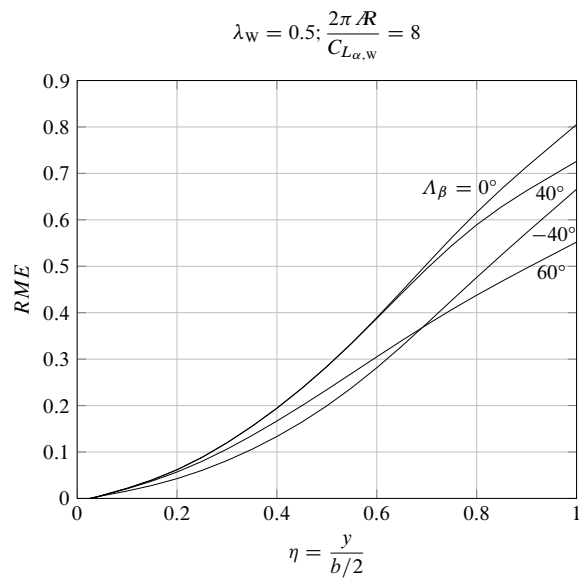
Figure 2.12. Rolling Moment Effectiveness for different geometries of the wing ($\lambda_W = 0$)



(a)

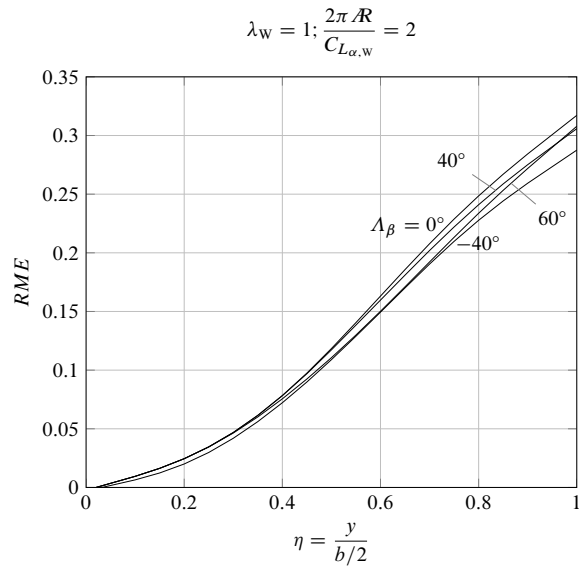


(b)

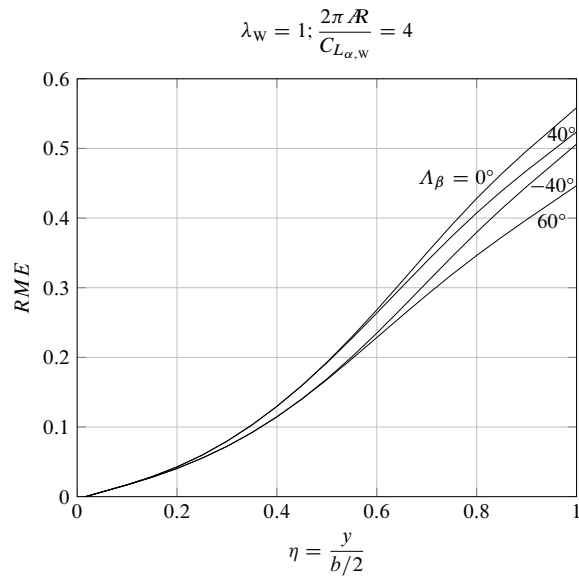


(c)

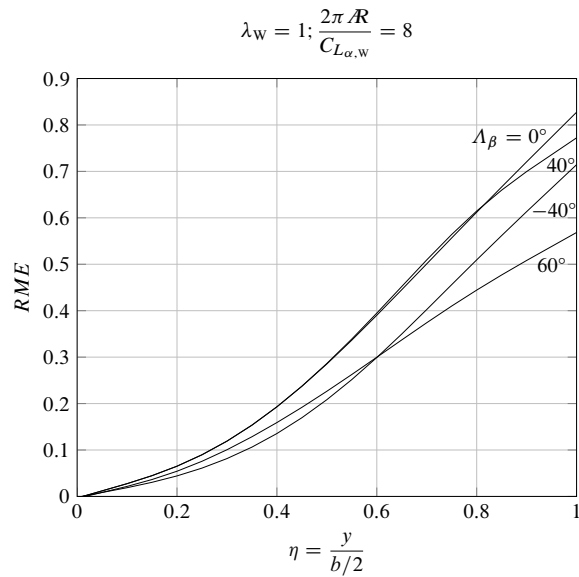
Figure 2.13. Rolling Moment Effectiveness for different geometries of the wing ($\lambda_w = 0.5$)



(a)



(b)



(c)

Figure 2.14. Rolling Moment Effectiveness for different geometries of the wing ($\lambda_W = 1$)

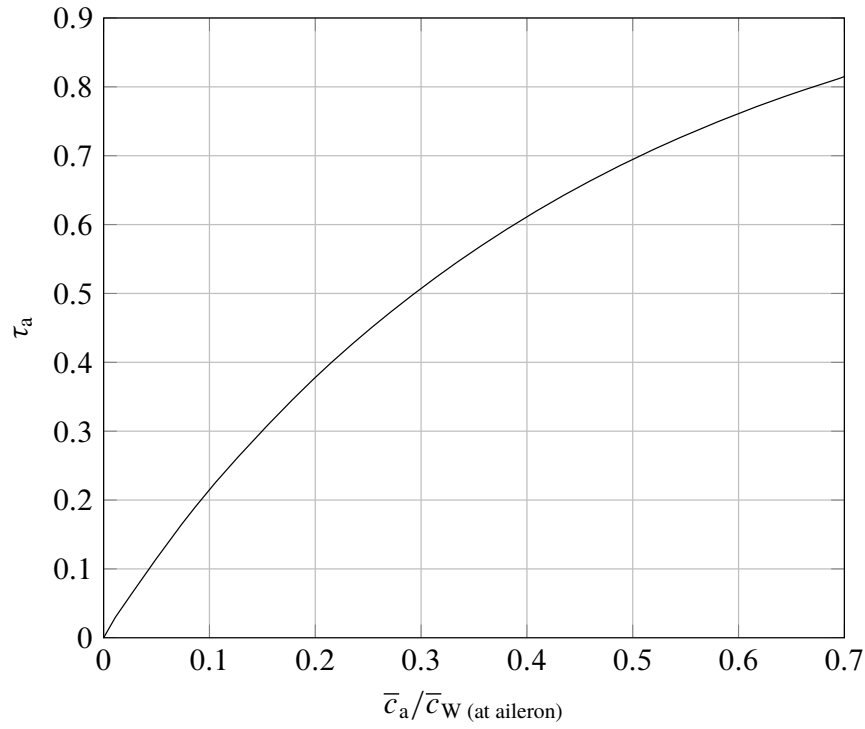


Figure 2.15. Effectiveness of the aileron τ_a as function of \bar{c}_a/\bar{c}_W (at aileron)

2.2.3 Rudder deflection effect

The rudder is the control surface, hinged at the tip of the vertical tail, which provides yaw control. Its contribution to the rolling moment originates from the lateral force associated with its deflection through its moment arm with respect to the aircraft centre of gravity. A mathematical relationship for this moment coefficient is:

$$C_{\mathcal{L}_{\delta_r}} = C_{Y_{\delta_r}} \frac{Z_r \cos \alpha_B - X_r \sin \alpha_B}{b_W} = |C_{L_{\alpha, v}}| \eta_V \frac{S_V}{S_W} \Delta(K_r) \tau_r \frac{Z_r \cos \alpha_B - X_r \sin \alpha_B}{b_W} \quad (2.24)$$

2.3 Steady-state yawing moment coefficient

The steady-state yawing moment can be evaluated by the relationship:

$$\mathcal{N} = C_{\mathcal{N}} \bar{q} S_W b_W \quad (2.25)$$

where the rolling moment coefficient can be expressed by:

$$C_{\mathcal{N}} = f(\beta, \delta_a, \delta_r) \quad (2.26)$$

The first order approximation for the Taylor expansion gives the following expression for $C_{\mathcal{N}}$:

$$C_{\mathcal{N}} = C_{\mathcal{N}_0} + C_{\mathcal{N}_\beta} \beta + C_{\mathcal{N}_{\delta_a}} \delta_a + C_{\mathcal{N}_{\delta_r}} \delta_r \quad (2.27)$$

in which the term $C_{\mathcal{N}_0}$ is zero if the aircraft is symmetric with respect to the XZ plane.

2.3.1 Weathercock effect

The aerodynamic coefficient C_{N_β} is known as weathercock effect and it can be expressed through its dependencies as shown in the following formula:

$$C_{N_\beta} = C_{N_\beta,W} + C_{N_\beta,B} + C_{N_\beta,H} + C_{N_\beta,V} \quad (2.28)$$

The contribution of the wing and the horizontal tail are negligible for all configurations. The fuselage contribution is evaluated using the relationship:

$$C_{N_\beta,B} = -57.3 K_N K_{ReB} \frac{S_{B,side}}{S_W} \frac{l_B}{b_W} \quad (2.29)$$

where the coefficient K_N is an empirical factor, given by figure 2.16 and related to the geometric coefficients of the axial cross section of the fuselage, whereas the coefficient K_{ReB} , given by figure 2.17 on the next page, is related to the fuselage Reynolds number.

The most significant contribution to C_{N_β} is provided by the vertical tail. This contribution is evaluated by:

$$\begin{aligned} C_{N_\beta,V} &= -C_{Y_\beta,V} \frac{Z_V \sin \alpha_B + X_V \cos \alpha_B}{b_W} = \\ &= k_{Y_V} |C_{L_{\alpha,V}}| \eta_V \left(1 - \frac{d\sigma}{d\beta} \right) \frac{S_V}{S_W} \frac{Z_V \sin \alpha_B + X_V \cos \alpha_B}{b_W} \end{aligned} \quad (2.30)$$

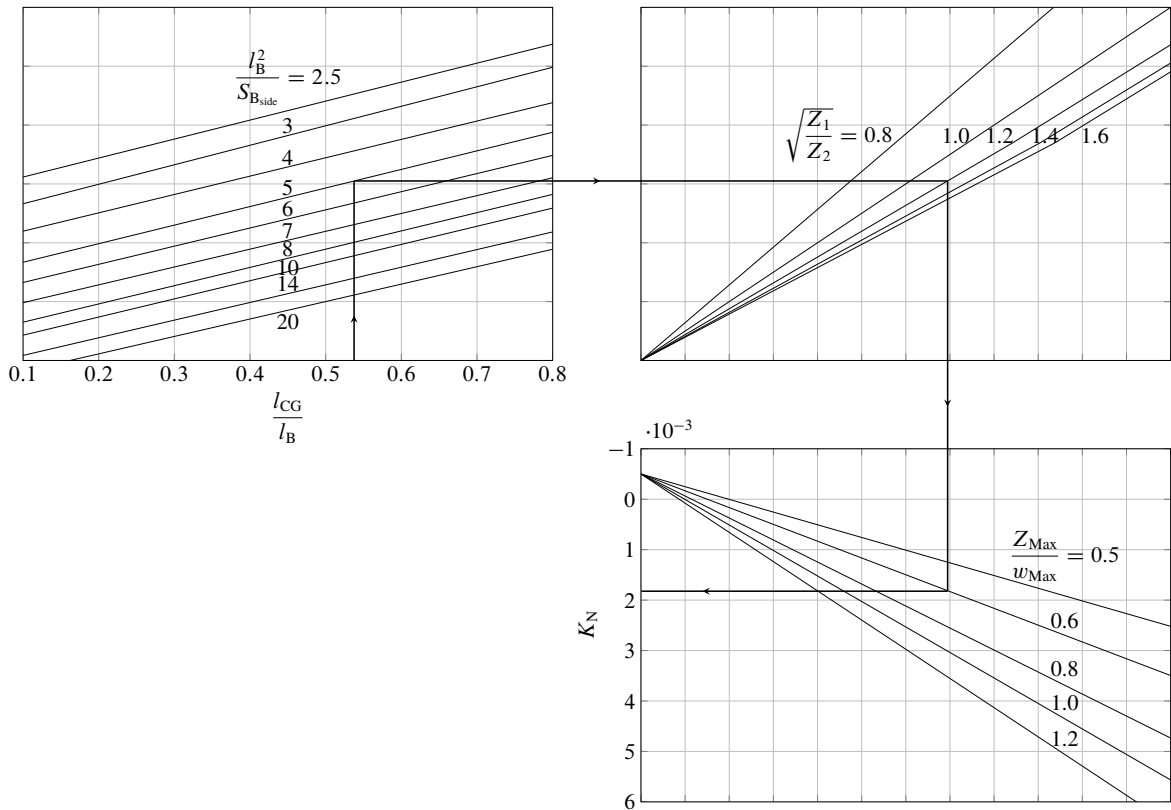


Figure 2.16. Empirical factor K_N for wing-body interface

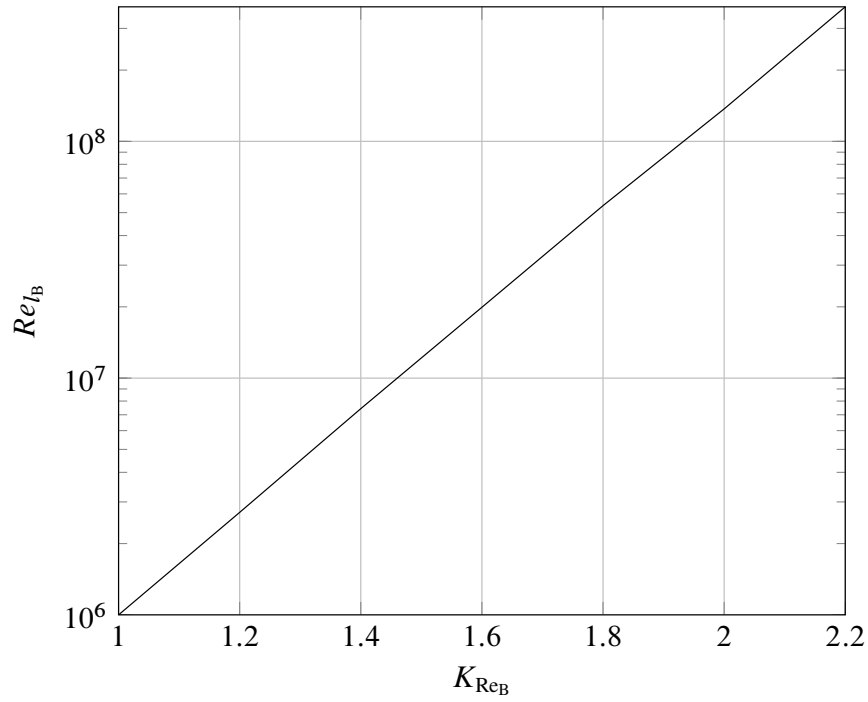


Figure 2.17. Effect of Reynolds number on wing-body interface

2.3.2 Ailerons deflection effect

The asymmetric deflection of the left and right ailerons also generate small but not negligible drag force leading to a small positive yawing moment. A relationship for modelling $C_{N_{\delta_a}}$ is given by:

$$C_{N_{\delta_a}} = -\Delta(K_{N_a})C_L C_{\mathcal{L}_{\delta_a}} \quad (2.31)$$

where C_L is the aircraft lift coefficient, the term $C_{\mathcal{L}_{\delta_a}}$ is the rolling moment coefficient due to ailerons deflection and K_{N_a} is evaluated from graphs of figure 2.18 on the following page.

2.3.3 Rudder deflection effect

This coefficient is related to the contribution given by the rudder deflection. The mathematical expression is:

$$\begin{aligned} C_{N_{\delta_r}} &= -C_{Y_{\delta_r}} \frac{Z_r \sin \alpha_B + X_r \cos \alpha_B}{b_W} = \\ &= -|C_{L_{\alpha_v}}| \eta_V \frac{S_V}{S_W} \Delta(K_r) \tau_r \frac{Z_r \sin \alpha_B + X_r \cos \alpha_B}{b_W} \end{aligned} \quad (2.32)$$

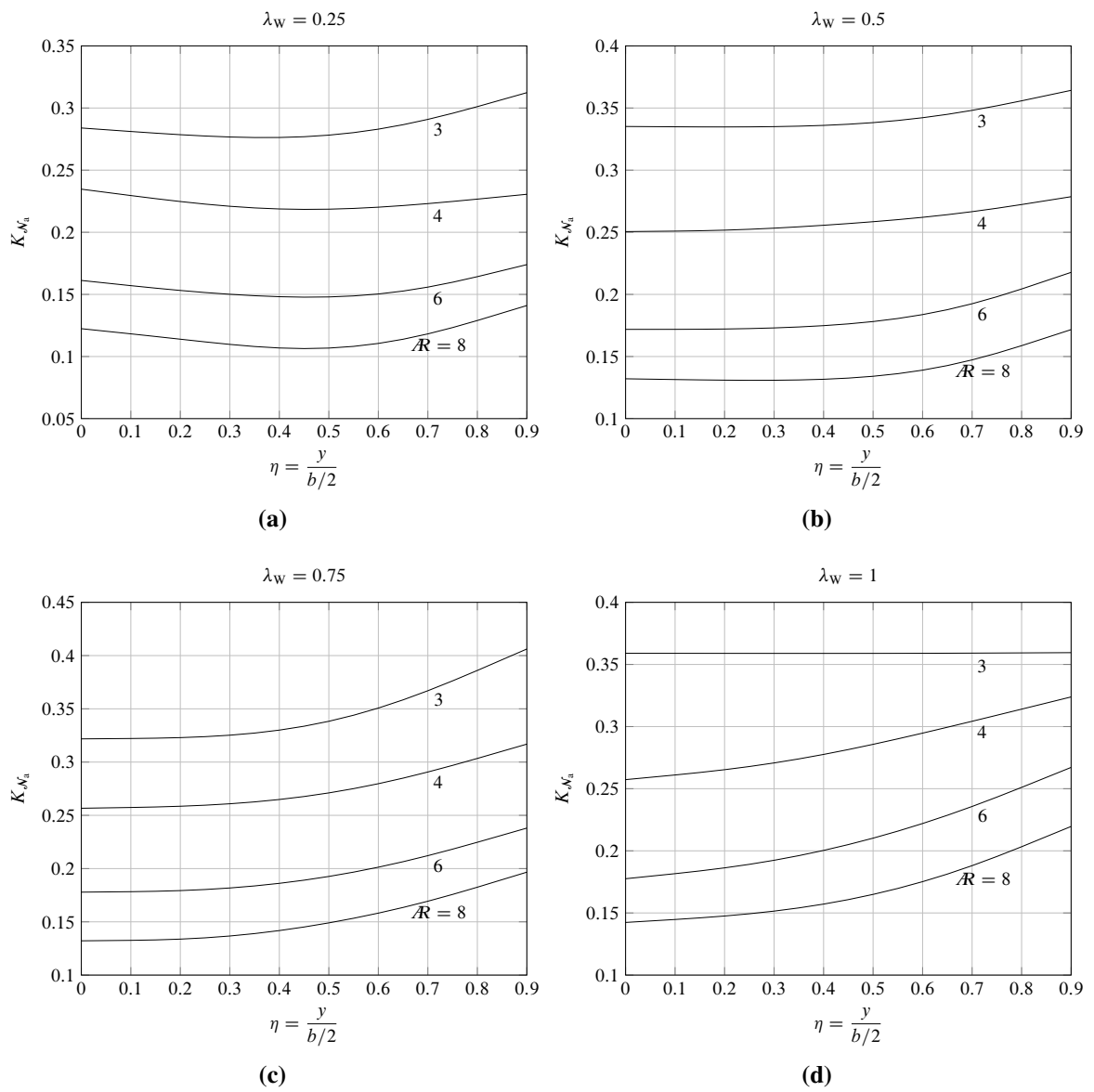


Figure 2.18. Correlation coefficient for yawing moment due to deflection of ailerons

2.4 Unsteady-state lateral force coefficient

2.4.1 Roll rate effect

The coefficient C_{Y_p} models the contribution of the lateral force coefficient due to roll rate. The vertical tail is the only component of the aircraft contributing to C_{Y_p} . The mathematical relationship is given by:

$$\begin{aligned} C_{Y_p} \approx C_{Y_{p,v}} &= 2C_{Y_{\beta,v}} \frac{Z_v \cos \alpha_B - X_v \sin \alpha_B}{b_w} = \\ &= -2k_{Y_v} |C_{L_{\alpha,v}}| \eta_v \left(1 - \frac{d\sigma}{d\beta}\right) \frac{S_v}{S_w} \frac{Z_v \cos \alpha_B - X_v \sin \alpha_B}{b_w} \end{aligned} \quad (2.33)$$

2.4.2 Yaw rate effect

The coefficient C_{Y_r} models the contribution of the lateral force coefficient due to yaw rate. As for C_{Y_p} , the vertical tail is the only component of the aircraft contributing to C_{Y_r} . The mathematical relationship is given by:

$$\begin{aligned} C_{Y_r} \approx C_{Y_{r,v}} &= -2C_{Y_{\beta,v}} \frac{Z_v \sin \alpha_B + X_v \cos \alpha_B}{b_w} = \\ &= 2k_{Y_v} |C_{L_{\alpha,v}}| \eta_v \left(1 - \frac{d\sigma}{d\beta}\right) \frac{S_v}{S_w} \frac{Z_v \sin \alpha_B + X_v \cos \alpha_B}{b_w} \end{aligned} \quad (2.34)$$

2.5 Unsteady-state rolling moment coefficient

2.5.1 Roll rate effect

The coefficient $C_{\mathcal{L}_p}$ models the contribution of the rolling moment coefficient due to roll rate. The mathematical relationship is given by:

$$C_{\mathcal{L}_p} = C_{\mathcal{L}_{p,wb}} + C_{\mathcal{L}_{p,H}} + C_{\mathcal{L}_{p,v}} \quad (2.35)$$

The contribution of the fuselage is negligible, so $C_{\mathcal{L}_{p,wb}} \approx C_{\mathcal{L}_{p,w}}$, and the relationship for this coefficient is given by:

$$C_{\mathcal{L}_{p,w}} = RDP \frac{k}{\sqrt{1 - M^2}} \quad (2.36)$$

where RDP is the rolling damping parameter, evaluated from graphs of figure 2.19 on the next page.

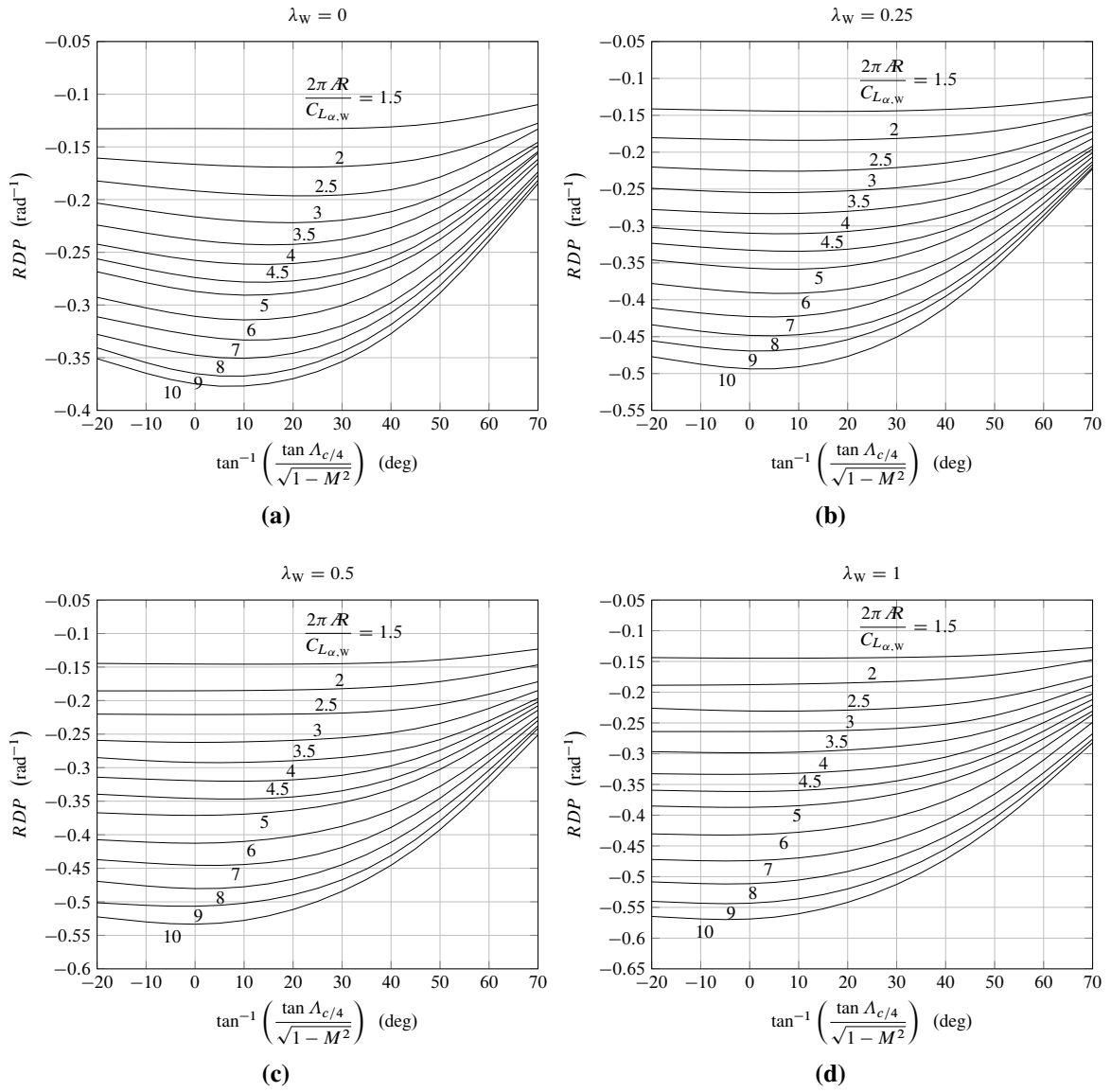


Figure 2.19. Rolling Damping Parameters for different wing geometry

A relationship for $C_{\mathcal{L}_{p,H}}$ is given by:

$$C_{\mathcal{L}_{p,H}} = \frac{1}{2} C_{\mathcal{L}_{p,w}} \bigg|_H \frac{S_H}{S_W} \left(\frac{b_H}{b_W} \right)^2 \quad (2.37)$$

where the $C_{\mathcal{L}_{p,w}} \big|_H$ is the previously introduced $C_{\mathcal{L}_{p,w}}$ evaluated with the geometric parameters of the horizontal tail. This coefficient is often negligible due to the low numerical value of the product of $S_H/S_W \cdot (b_H/b_W)^2$.

The contribution of the vertical tail is:

$$C_{\mathcal{L}_{p,v}} = 2C_{Y_{\beta,v}} \left(\frac{Z_v}{b_w} \right)^2 = -2k_{Y_v} |C_{L_{\alpha,v}}| \eta_v \left(1 - \frac{d\sigma}{d\beta} \right) \frac{S_v}{S_w} \left(\frac{Z_v}{b_w} \right)^2 \quad (2.38)$$

2.5.2 Yaw rate effect

The contribution to the rolling moment due to the yaw rate is contained in the coefficient $C_{\mathcal{L}_r}$. The modelling for this coefficient starts from the following relationship:

$$C_{\mathcal{L}_r} = C_{\mathcal{L}_r, \text{WB}} + C_{\mathcal{L}_r, \text{H}} + C_{\mathcal{L}_r, \text{V}} \quad (2.39)$$

The fuselage and the horizontal tail do not significantly contribute to this coefficient, so we have $C_{\mathcal{L}_r} \approx C_{\mathcal{L}_r, \text{W}} + C_{\mathcal{L}_r, \text{V}}$.

The wing contribution is given by:

$$C_{\mathcal{L}_r, \text{W}} = \left(\frac{C_{\mathcal{L}_r}}{C_L} \right) \Big|_{C_L=0} C_L + \left(\frac{\Delta C_{\mathcal{L}_r}}{\Gamma_{\text{W}}} \right) \Gamma_{\text{W}} + \left(\frac{\Delta C_{\mathcal{L}_r}}{\varepsilon_{\text{W}}} \right) \varepsilon_{\text{W}} \quad (2.40)$$

The coefficient $\left(C_{\mathcal{L}_r}/C_L \right) \Big|_{C_L=0}$ is given by:

$$\left(\frac{C_{\mathcal{L}_r}}{C_L} \right) \Big|_{C_L=0} = D \left(\frac{C_{\mathcal{L}_r}}{C_L} \right) \Big|_{M=0, C_L=0} \quad (2.41)$$

where:

$$D = \frac{1 + \frac{\mathcal{R}_{\text{W}}(1 - B^2)}{2B[\mathcal{R}_{\text{W}}B + 2 \cos \Lambda_{c/4}]} + \frac{\mathcal{R}_{\text{W}}B + 2 \cos \Lambda_{c/4} \tan^2 \Lambda_{c/4}}{\mathcal{R}_{\text{W}}B + 4 \cos \Lambda_{c/4} \frac{8}{8}}}{1 + \frac{\mathcal{R}_{\text{W}} + 2 \cos \Lambda_{c/4} \tan^2 \Lambda_{c/4}}{\mathcal{R}_{\text{W}} + 4 \cos \Lambda_{c/4} \frac{8}{8}}} \quad (2.42)$$

in which:

$$B = \sqrt{1 - M^2 \cos^2 \Lambda_{c/4}} \quad (2.43)$$

and $\left(C_{\mathcal{L}_r}/C_L \right) \Big|_{M=0, C_L=0}$ is given by figure 2.20 on the following page. In the equation 2.40 the term $\Delta C_{\mathcal{L}_r}/\Gamma_{\text{W}}$ is a factor due to the wing dihedral angle, whereas the term $\Delta C_{\mathcal{L}_r}/\varepsilon_{\text{W}}$ is a factor due to the wing twist angle. The first factor is modelled using the relationship:

$$\frac{\Delta C_{\mathcal{L}_r}}{\Gamma_{\text{W}}} = \frac{1}{12} \frac{\pi \mathcal{R}_{\text{W}} \sin \Lambda_{c/4}}{\mathcal{R}_{\text{W}} + 4 \cos \Lambda_{c/4}} \quad (2.44)$$

the second one is evaluated using figure 2.21 on the next page.

The vertical tail contribution into the equation 2.39 is given by:

$$\begin{aligned} C_{\mathcal{L}_r, \text{V}} &= -2C_{Y_{\beta, \text{V}}} \frac{Z_{\text{V}} \sin \alpha_{\text{B}} + X_{\text{V}} \cos \alpha_{\text{B}}}{b_{\text{W}}} \frac{Z_{\text{V}} \cos \alpha_{\text{B}} - X_{\text{V}} \sin \alpha_{\text{B}}}{b_{\text{W}}} = \\ &= 2k_{Y_{\text{V}}} |C_{L_{\alpha, \text{V}}}| \eta_{\text{V}} \left(1 - \frac{d\sigma}{d\beta} \right) \frac{S_{\text{V}}}{S_{\text{W}}} \frac{Z_{\text{V}} \sin \alpha_{\text{B}} + X_{\text{V}} \cos \alpha_{\text{B}}}{b_{\text{W}}} \frac{Z_{\text{V}} \cos \alpha_{\text{B}} - X_{\text{V}} \sin \alpha_{\text{B}}}{b_{\text{W}}} \end{aligned} \quad (2.45)$$

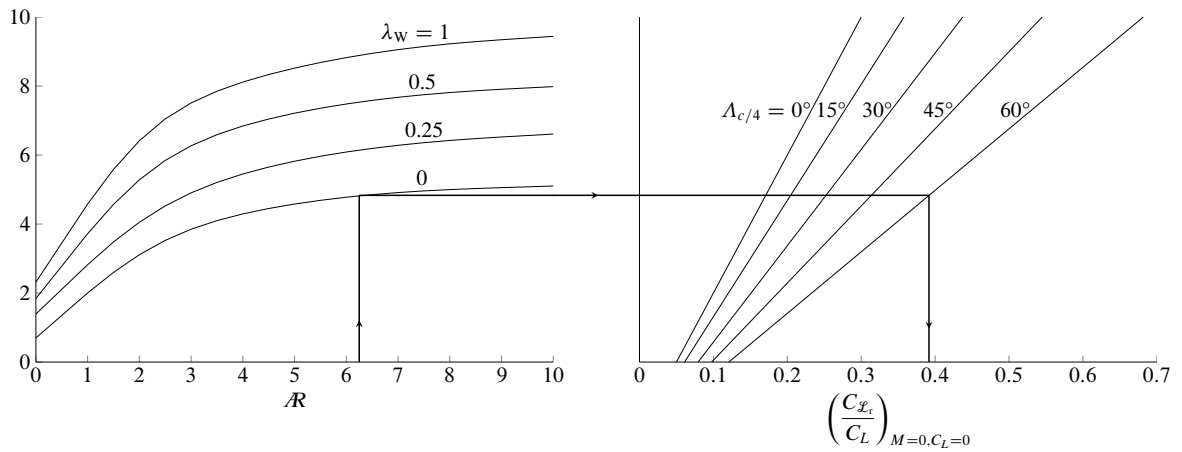


Figure 2.20. Evaluation of $\left(\frac{C_{\mathcal{L}_r}}{C_L}\right)_{M=0, C_L=0}$

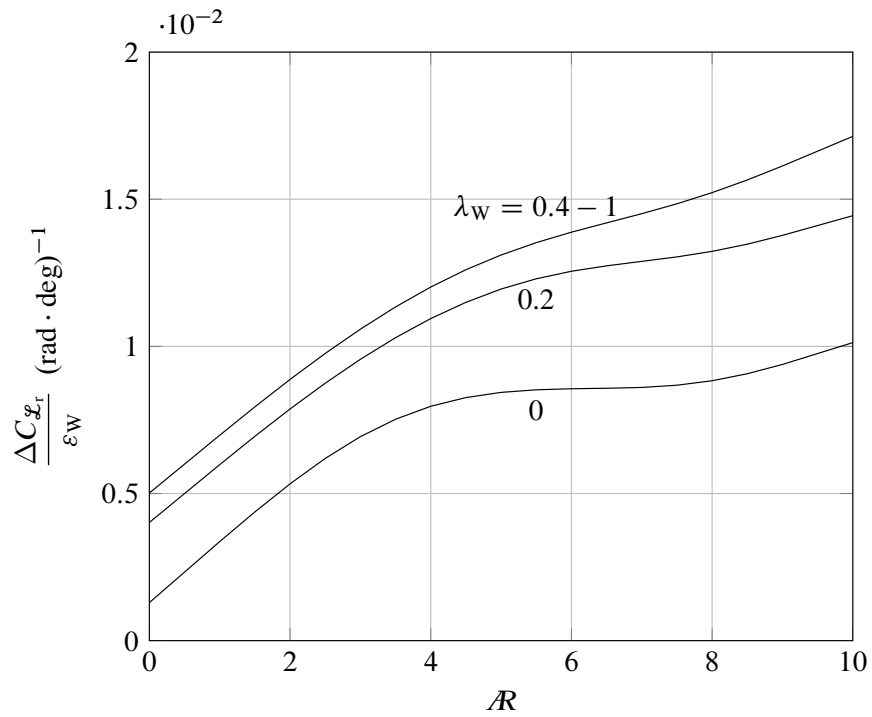


Figure 2.21. Effect of wing twist on $C_{\mathcal{L}_r}$.

2.6 Unsteady-state yawing moment coefficient

2.6.1 Roll rate effect

The coefficient $C_{\mathcal{N}_p}$ models the contribution to the yawing moment due to the roll rate. The relationship for this coefficient is:

$$C_{\mathcal{N}_p} = C_{\mathcal{N}_{p, \text{WB}}} + C_{\mathcal{N}_{p, \text{H}}} + C_{\mathcal{N}_{p, \text{V}}} \quad (2.46)$$

Because the fuselage and the horizontal tail do not significantly contribute to this coefficient, we have that $C_{\mathcal{N}_p} \approx C_{\mathcal{N}_{p, \text{W}}} + C_{\mathcal{N}_{p, \text{V}}}$.

A relationship for the wing contribution is given by:

$$C_{\mathcal{N}_{p, \text{W}}} = -C_{\mathcal{L}_{p, \text{W}}} \tan \alpha_B + C_{\mathcal{L}_p} \tan \alpha_B + \left(\frac{C_{\mathcal{N}_p}}{C_L} \right) \Big|_{C_L=0} C_L + \left(\frac{\Delta C_{\mathcal{N}_p}}{\varepsilon_W} \right) \varepsilon_W \quad (2.47)$$

where $C_{\mathcal{L}_{p, \text{W}}}$ and $C_{\mathcal{L}_p}$ are described in 2.36 and 2.35, respectively. The coefficient $\left(\frac{C_{\mathcal{N}_p}}{C_L} \right) \Big|_{C_L=0}$ is given by:

$$\left(\frac{C_{\mathcal{N}_p}}{C_L} \right) \Big|_{C_L=0} = C \left(\frac{C_{\mathcal{N}_p}}{C_L} \right) \Big|_{M=0, C_L=0} \quad (2.48)$$

where:

$$C = \frac{\mathcal{R}_W + 4 \cos \Lambda_{c/4}}{\mathcal{R}_W B + 4 \cos \Lambda_{c/4}} \frac{\mathcal{R}_W B + \frac{1}{2} [\mathcal{R}_W B + 4 \cos \Lambda_{c/4}] \tan^2 \Lambda_{c/4}}{\mathcal{R}_W + \frac{1}{2} [\mathcal{R}_W + 4 \cos \Lambda_{c/4}] \tan^2 \Lambda_{c/4}} \quad (2.49)$$

in which:

$$B = \sqrt{1 - M^2 \cos^2 \Lambda_{c/4}} \quad (2.50)$$

and $\left(\frac{C_{\mathcal{N}_p}}{C_L} \right) \Big|_{M=0, C_L=0}$ is modelled using the relationship:

$$\left(\frac{C_{\mathcal{N}_p}}{C_L} \right) \Big|_{M=0, C_L=0} = -\frac{1}{6} \frac{\mathcal{R}_W + 6(\mathcal{R}_W + \cos \Lambda_{c/4}) \left[(\bar{x}_{\text{CG}} - \bar{x}_{\text{AC}}) \frac{\tan \Lambda_{c/4}}{\mathcal{R}_W} + \frac{\tan^2 \Lambda_{c/4}}{12} \right]}{\mathcal{R}_W + \cos \Lambda_{c/4}} \quad (2.51)$$

The term $\Delta C_{\mathcal{N}_p} / \varepsilon_W$ is associated with the wing twist angle and is taken from figure 2.22 on the following page.

The vertical tail contribution into the equation 2.46 is given by:

$$\begin{aligned} C_{\mathcal{L}_{r, \text{V}}} &= -2C_{Y_{\beta, \text{V}}} \frac{Z_V \sin \alpha_B + X_V \cos \alpha_B}{b_W} \frac{Z_V \cos \alpha_B - X_V \sin \alpha_B - Z_V}{b_W} = \\ &= 2k_{Y_V} |C_{L_{\alpha, \text{V}}}| \eta_V \left(1 - \frac{d\sigma}{d\beta} \right) \frac{S_V}{S_W} \frac{Z_V \sin \alpha_B + X_V \cos \alpha_B}{b_W} \frac{Z_V \cos \alpha_B - X_V \sin \alpha_B - Z_V}{b_W} \end{aligned} \quad (2.52)$$

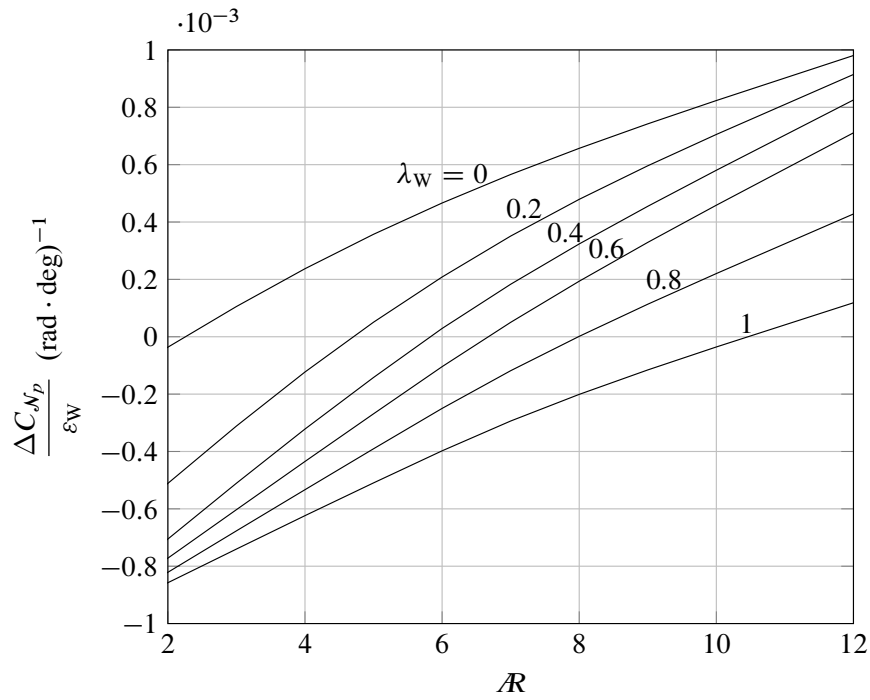


Figure 2.22. Effect of wing twist on C_{N_p}

2.6.2 Yaw rate effect

The coefficient C_{N_r} models the contribution to the yawing moment due to the yaw rate. A relationship for this coefficient is:

$$C_{N_r} = C_{N_{r,WB}} + C_{N_{r,H}} + C_{N_{r,V}} \quad (2.53)$$

The fuselage and the horizontal tail do not significantly contribute to this coefficient; therefore, we have that $C_{N_r} \approx C_{N_{r,W}} + C_{N_{r,V}}$.

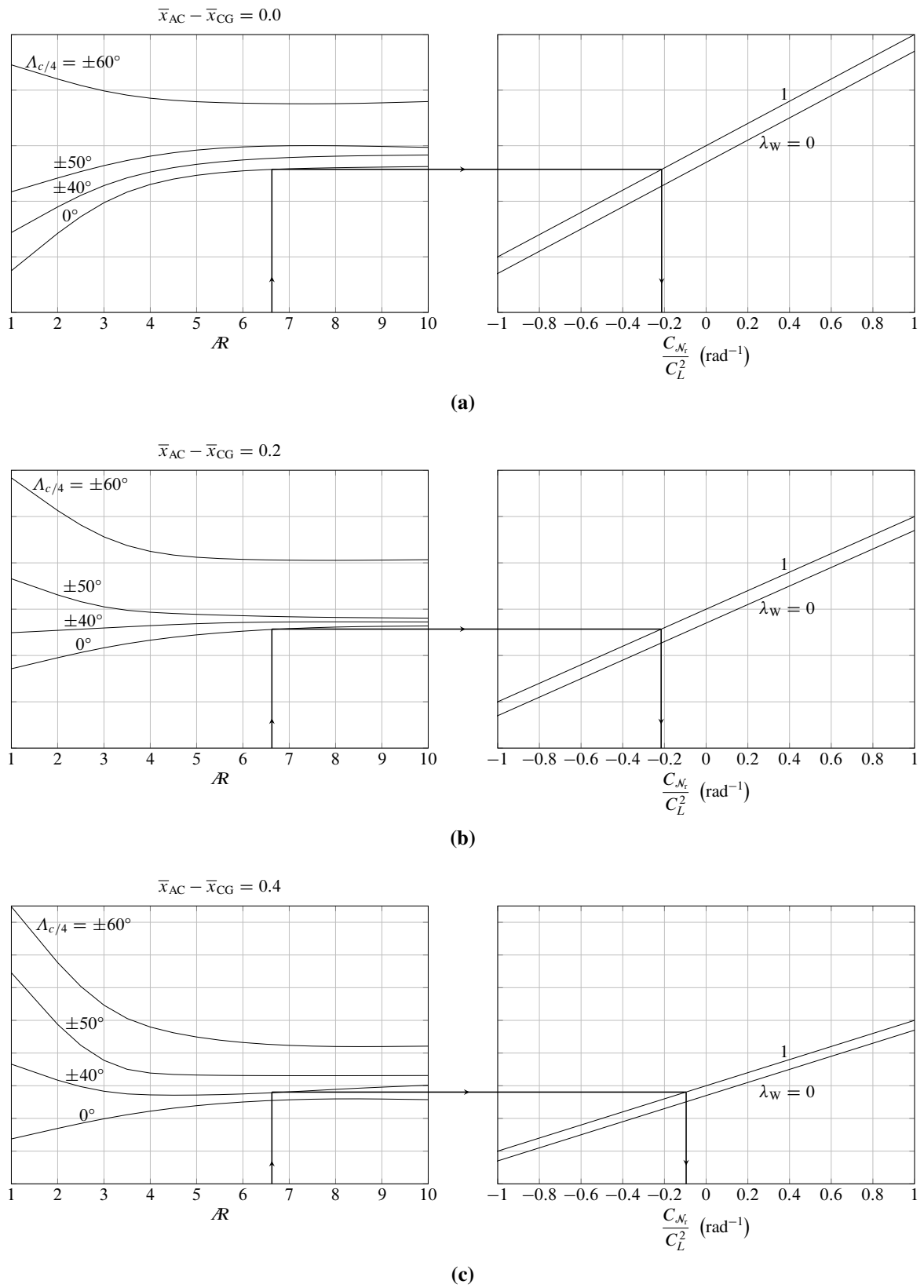
The wing contribution is evaluated by the relationship:

$$C_{N_{r,W}} = \left(\frac{C_{N_r}}{C_L^2} \right) C_L^2 + \left(\frac{C_{N_r}}{C_{D_0}} \right) C_{D_0} \quad (2.54)$$

in which the terms C_{N_r}/C_L^2 and C_{N_r}/C_{D_0} are evaluated from figure 2.23 on the next page and figure 2.24 on page 31 respectively.

The vertical tail contribution is given by:

$$\begin{aligned} C_{N_{r,V}} &= 2C_{Y_{\beta,V}} \left(\frac{Z_V \sin \alpha_B + X_V \cos \alpha_B}{b_W} \right)^2 = \\ &= -2k_{Y_V} |C_{L_{\alpha,V}}| \eta_V \left(1 - \frac{d\sigma}{d\beta} \right) \frac{S_V}{S_W} \left(\frac{Z_V \sin \alpha_B + X_V \cos \alpha_B}{b_W} \right)^2 \end{aligned} \quad (2.55)$$

Figure 2.23. Effect of lift on C_{N_r}

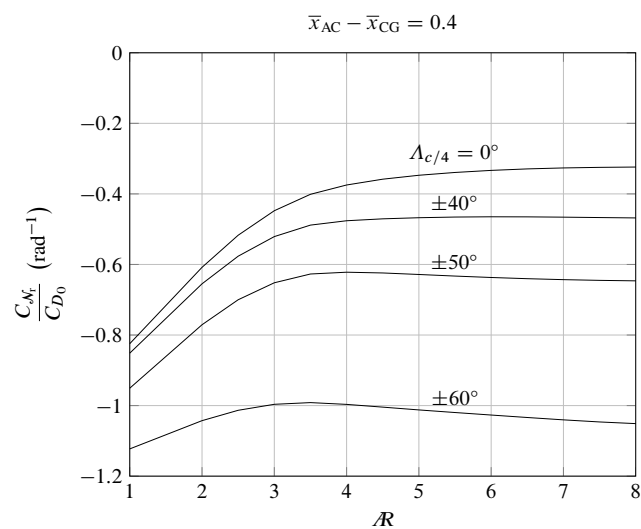
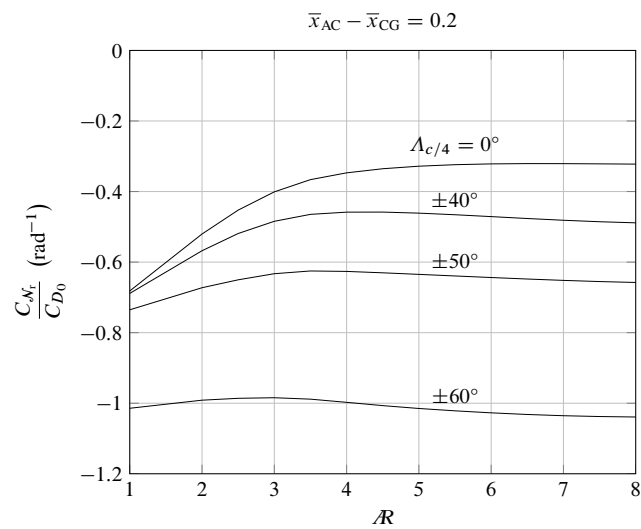
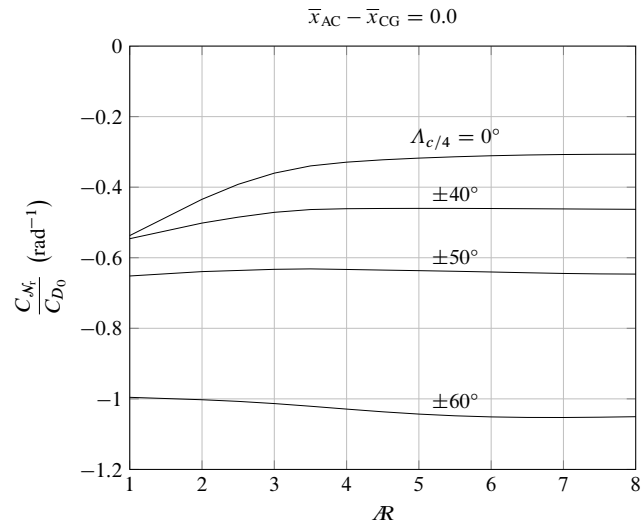


Figure 2.24. Effect of parasite drag on C_{N_r}

Example of application on a regional turboprop

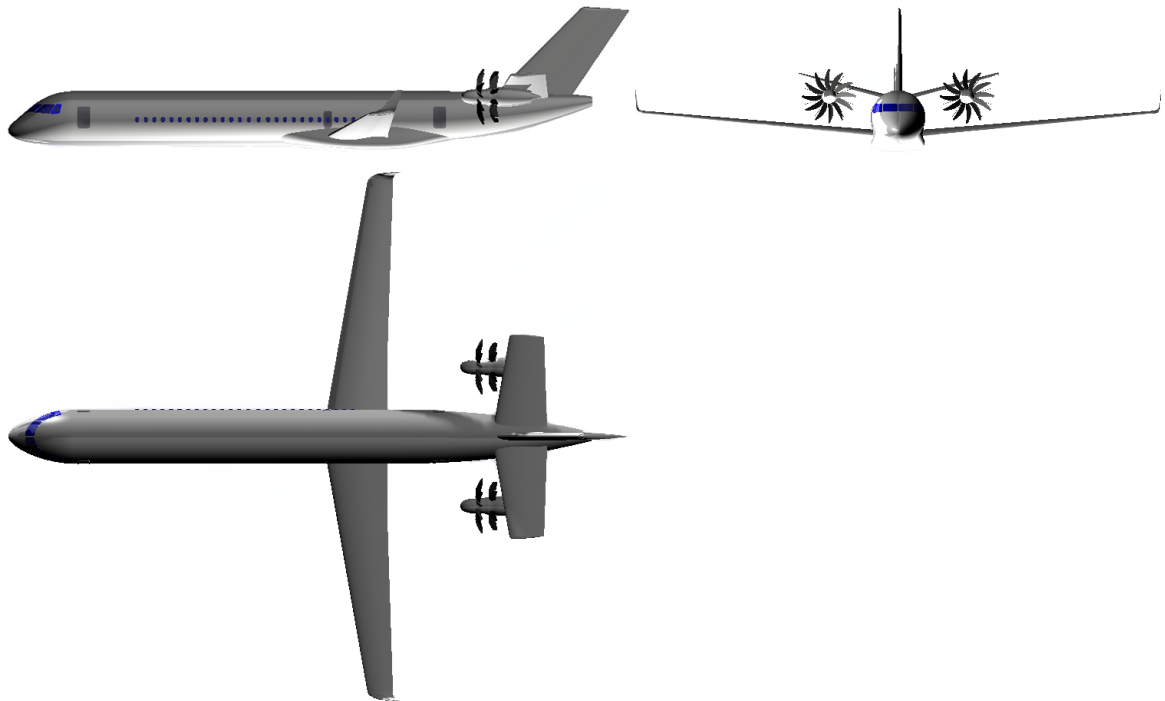


Figure 3.1. Three views of the aircraft

Table 3.1. Aircraft data

Variable	SI units	USCS units
C_{D_0}	0.03035	—
\bar{x}_{CG}	0.1	—
SSM	−0.080	—

Table 3.2. Flight conditions

Variable	SI units	USCS units
α_B	0 rad	0 deg
C_L	0.650	—
M	0.640	—

Table 3.3. Wing related parameters

Variable	SI units	USCS units
S_W	98.60 m ²	1061.32 ft ²
b_W	34.34 m	112.66 ft
\mathcal{R}_W	11.961	—
λ_W	0.383	—
$\Lambda_{c/4,W}$	0.10159 rad	5.821 deg
$\Lambda_{c/2,W}$	0.02755 rad	1.578 deg
Γ_W	0.09599 rad	5.5 deg
ε_W	−0.03491 rad	−2 deg
$C_{L\alpha,w}$	6.342 rad ^{−1}	0.11068 deg ^{−1}
Z_W	1.33 m	4.36 ft
$\eta_{a,IN}$	0.78	—
$\eta_{a,OUT}$	0.95	—
\bar{c}_a/\bar{c}_W (at aileron)	0.32	—
τ_a	0.530	—

Table 3.4. Fuselage related parameters

Variable	SI units	USCS units
$S_{P \rightarrow V}$	6.77 m ²	72.85 ft ²
$S_{B,side}$	108.46 m ²	1167.45 ft ²
Re_B	2.35E8	—
$d_{W,B}$	3.54 m	11.60 ft
$d_{W,H}$	2.46 m	8.07 ft
d	3.56 m	11.69 ft
l_B	38.04 m	124.80 ft
w_{max}	3.51 m	11.52 ft
Z_{max}	3.56 m	11.69 ft
Z_1	3.56 m	11.69 ft
Z_2	3.46 m	11.34 ft
r_1	2.60 m	8.53 ft

Table 3.5. Horizontal tail related parameters

Variable	SI units	USCS units
S_H	39.91 m ²	429.59 ft ²
b_H	13.04 m	42.78 ft
AR_H	4.261	—
λ_H	0.624	—
$\Lambda_{c/4,H}$	0.07485 rad	4.286 deg
$\Lambda_{c/2,H}$	-0.02633 rad	-1.509 deg
Γ_H	0.26180 rad	15 deg
ε_H	0 rad	0 deg
$C_{L\alpha,H}$	4.261 rad ⁻¹	0.07437 deg ⁻¹
η_H	0.8	—

Table 3.6. Vertical tail related parameters

Variable	SI units	USCS units
S_V	24.45 m ²	263.18 ft ²
b_V	5.78 m	18.96 ft
λ_V	0.640	—
X_V	13.17 m	43.21 ft
Z_V	1.52 m	4.99 ft
$C_{L\alpha,V}$	2.079 rad ⁻¹	0.03629 deg ⁻¹
η_V	0.9	—
$\eta_{r,IN}$	0	—
$\eta_{r,OUT}$	0.9	—
\bar{c}_r/\bar{c}_V	0.35	—
τ_r	0.562	—
X_r	15.21 m	49.90 ft
Z_r	4.12 m	13.52 ft

Table 3.7. Outcome parameters from lateral-directional calculations – Steady coefficients

Variable	SI units	USCS units
C_{Y_0}	0	—
$C_{Y_{\beta,W}}$	-0.032 rad^{-1}	$-0.00056 \text{ deg}^{-1}$
$C_{Y_{\beta,B}}$	-0.154 rad^{-1}	$-0.00269 \text{ deg}^{-1}$
$C_{Y_{\beta,H}}$	-0.056 rad^{-1}	$-0.00098 \text{ deg}^{-1}$
$C_{Y_{\beta,V}}$	-0.533 rad^{-1}	$-0.00930 \text{ deg}^{-1}$
$C_{Y_{\beta}}$	-0.774 rad^{-1}	$-0.01351 \text{ deg}^{-1}$
$C_{Y_{\delta_a}}$	0 rad^{-1}	0 deg^{-1}
$C_{Y_{\delta_r}}$	0.251 rad^{-1}	0.00438 deg^{-1}
$C_{\mathcal{L}_0}$	0	—
$C_{\mathcal{L}_{\beta,WB}}$	-0.056 rad^{-1}	$-0.00098 \text{ deg}^{-1}$
$C_{\mathcal{L}_{\beta,H}}$	-0.024 rad^{-1}	$-0.00042 \text{ deg}^{-1}$
$C_{\mathcal{L}_{\beta,V}}$	-0.024 rad^{-1}	$-0.00042 \text{ deg}^{-1}$
$C_{\mathcal{L}_{\beta}}$	-0.104 rad^{-1}	$-0.00182 \text{ deg}^{-1}$
$C_{\mathcal{L}_{\delta_a}}$	-0.052 rad^{-1}	$-0.00091 \text{ deg}^{-1}$
$C_{\mathcal{L}_{\delta_r}}$	0.030 rad^{-1}	0.00052 deg^{-1}
$C_{\mathcal{N}_0}$	0	—
$C_{\mathcal{N}_{\beta,B}}$	-0.167 rad^{-1}	$-0.00292 \text{ deg}^{-1}$
$C_{\mathcal{N}_{\beta,V}}$	0.205 rad^{-1}	0.00357 deg^{-1}
$C_{\mathcal{N}_{\beta}}$	0.038 rad^{-1}	0.00065 deg^{-1}
$C_{\mathcal{N}_{\delta_a}}$	0 rad^{-1}	0 deg^{-1}
$C_{\mathcal{N}_{\delta_r}}$	-0.111 rad^{-1}	$-0.00194 \text{ deg}^{-1}$

Table 3.8. Outcome parameters from lateral-directional calculations – Unsteady coefficients

Variable	SI units	USCS units
C_{Y_p}	-0.047 rad^{-1}	$-0.00082 \text{ deg}^{-1}$
C_{Y_r}	0.409 rad^{-1}	0.00714 deg^{-1}
$C_{\mathcal{L}_{p,WB}}$	-0.522 rad^{-1}	$-0.00911 \text{ deg}^{-1}$
$C_{\mathcal{L}_{p,H}}$	-0.009 rad^{-1}	$-0.00016 \text{ deg}^{-1}$
$C_{\mathcal{L}_{p,V}}$	-0.002 rad^{-1}	$-0.00005 \text{ deg}^{-1}$
$C_{\mathcal{L}_p}$	-0.533 rad^{-1}	$-0.00932 \text{ deg}^{-1}$
$C_{\mathcal{L}_{r,W}}$	0.175 rad^{-1}	0.00305 deg^{-1}
$C_{\mathcal{L}_{r,V}}$	0.018 rad^{-1}	0.00031 deg^{-1}
$C_{\mathcal{L}_r}$	0.193 rad^{-1}	0.00336 deg^{-1}
$C_{\mathcal{N}_{p,W}}$	-0.095 rad^{-1}	$-0.00166 \text{ deg}^{-1}$
$C_{\mathcal{N}_{p,V}}$	0 rad^{-1}	0 deg^{-1}
$C_{\mathcal{N}_p}$	-0.095 rad^{-1}	$-0.00166 \text{ deg}^{-1}$
$C_{\mathcal{N}_{r,W}}$	-0.017 rad^{-1}	$-0.00029 \text{ deg}^{-1}$
$C_{\mathcal{N}_{r,V}}$	0.084 rad^{-1}	0.00146 deg^{-1}
$C_{\mathcal{N}_r}$	0.067 rad^{-1}	0.00117 deg^{-1}

HDF dataset and database reader creation

In a tool for preliminary design phase of an aircraft, it's very important to have available database. It's possible to create database starting from graphics using external software. In this appendix will be explained the step required in order to digitalize the graphics, create an HDF dataset and set up the database-reader class in JPAD.

A.1 Chart digitization

The first step required for create a dataset is to digitalize a chart. Often data are presented in reports and references as functional X-Y type scatter or line plots. In order to use this data, it must somehow be digitized. This is made with a MATLAB tool, such as *GrabIt*. GrabIt is a Java program used to digitize scanned plots of functional data. This program will allow you to take a scanned image of a plot and quickly digitize values off the plot just by clicking the mouse on each data point [1].

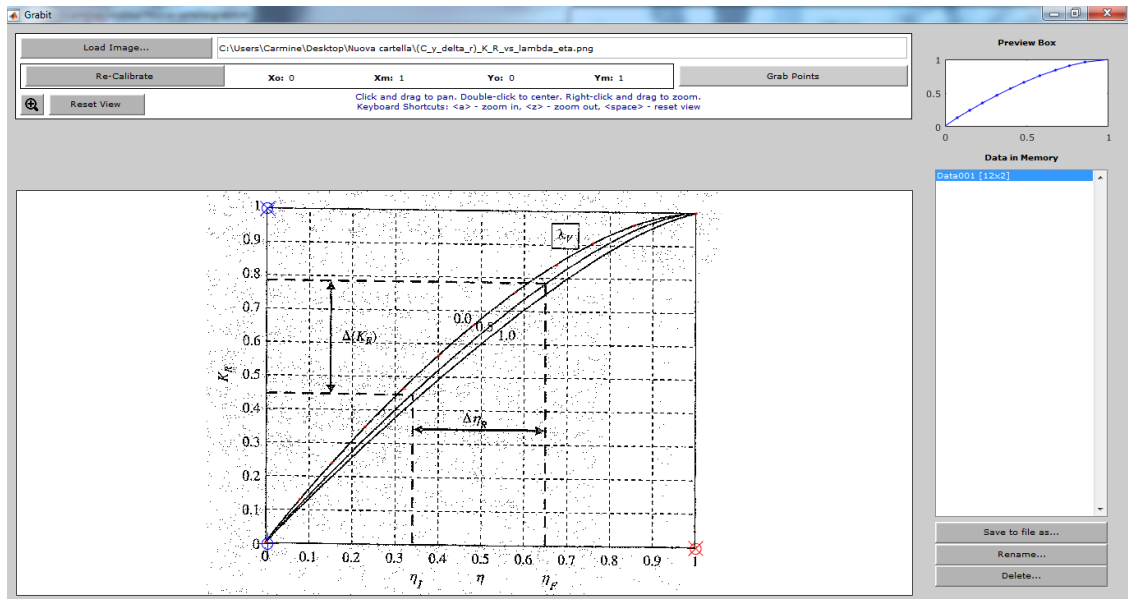


Figure A.1. Chart digitization using GrabIt

In order to digitize a chart, first of all it's necessary to calibrate the axis. GrabIt works with both linear and logarithmic axis scales. After it's possible to digitize a curve simply click on it. The values obtained can then be saved to .mat file (MATLAB data).

A.2 Creation of an HDF file with MATLAB

Obtained the .mat file from digitization is necessary to create the HDF file. After saving the imported files as .mat file, MATLAB code comes in play to manage these data and to generate the digitalized curves and the HDF dataset. The code interpolates curves points with cubic splines in order to have more points to plot for each curve.

Listing A.1. MATLAB script for creating the HDF database

```
clear; close all; clc;
%% Load data file generated by Grabit
% https://it.mathworks.com/matlabcentral/fileexchange/7173-grabit

fileBaseNames = {'KR_vs_lambda_eta_00', 'KR_vs_lambda_eta_05', 'KR_vs_lambda_eta_10'};
nPoints       = 21;
xx            = linspace(0.0, 1.0, nPoints);

for kFile = 1:length(fileBaseNames)

    s = load(fileBaseNames{kFile}, '-mat');

    %% Allocate imported array to column variable names
    x{kFile}      = s.(fileBaseNames{kFile})(:, 1);
    x{kFile}(1)   = 0.0;
    x{kFile}(end) = 1.0;

    y{kFile}      = s.(fileBaseNames{kFile})(:, 2);
    y{kFile}(1)   = 0.0;
    y{kFile}(end) = 1.0;

    %% Smoothing
    pp(kFile)     = csaps(x{kFile}, y{kFile}, 0.999999);
    c{kFile}      = ppval(pp(kFile), xx');
    data(:,kFile) = c{kFile};
    data(1,kFile) = 0.0;
    data(end,kFile) = 1.0;

    plot(xx', data(:,kFile), '-*');
    hold on
end
xlabel('$\eta$', 'interpreter', 'latex');
ylabel('$K_r$', 'interpreter', 'latex');
title('Span_factor_between_rudder_and_vertical_tail');
axis([0 1 0 1]);
legend('0.0', '0.5', '1.0');

%% Output to HDF
taperRatios = [0.0 0.5 1.0]';
etas        = xx';

hdfFileName = 'C_y_delta_r_K_R_vs_lambda_eta.h5';

if(exist(hdfFileName, 'file'))
    fprintf('file_exists,_deleting_and_creating_a_new_one\n', hdfFileName);
    delete(hdfFileName)
else
    fprintf('Creating_new_file_%s\n', hdfFileName);
end

h5create(hdfFileName, '/(C_y_delta_r)_K_R_vs_lambda_eta/data', size(data'));
h5write(hdfFileName, '/(C_y_delta_r)_K_R_vs_lambda_eta/data', data');

h5create(hdfFileName, '/(C_y_delta_r)_K_R_vs_lambda_eta/var_0', size(taperRatios'));
h5write(hdfFileName, '/(C_y_delta_r)_K_R_vs_lambda_eta/var_0', taperRatios');

h5create(hdfFileName, '/(C_y_delta_r)_K_R_vs_lambda_eta/var_1', size(etas'));
h5write(hdfFileName, '/(C_y_delta_r)_K_R_vs_lambda_eta/var_1', etas');
```

This script draws the graph after digitization (see figure A.2). In this way it's possible to compare the initial graph and the digitized one.

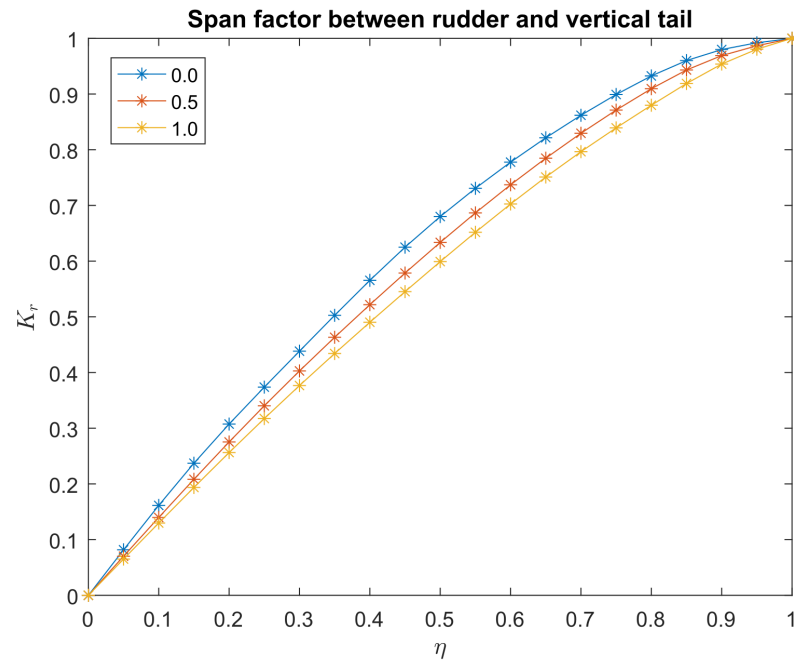


Figure A.2. Chart digitization plot

Having created the .h5 file it is necessary to import it in database using *HDFView* [6] and to set up the database reader implementing in specific class the variable declaration of an interpolating function starting from the .h5 file. In conclusion the getter method has to be defined.

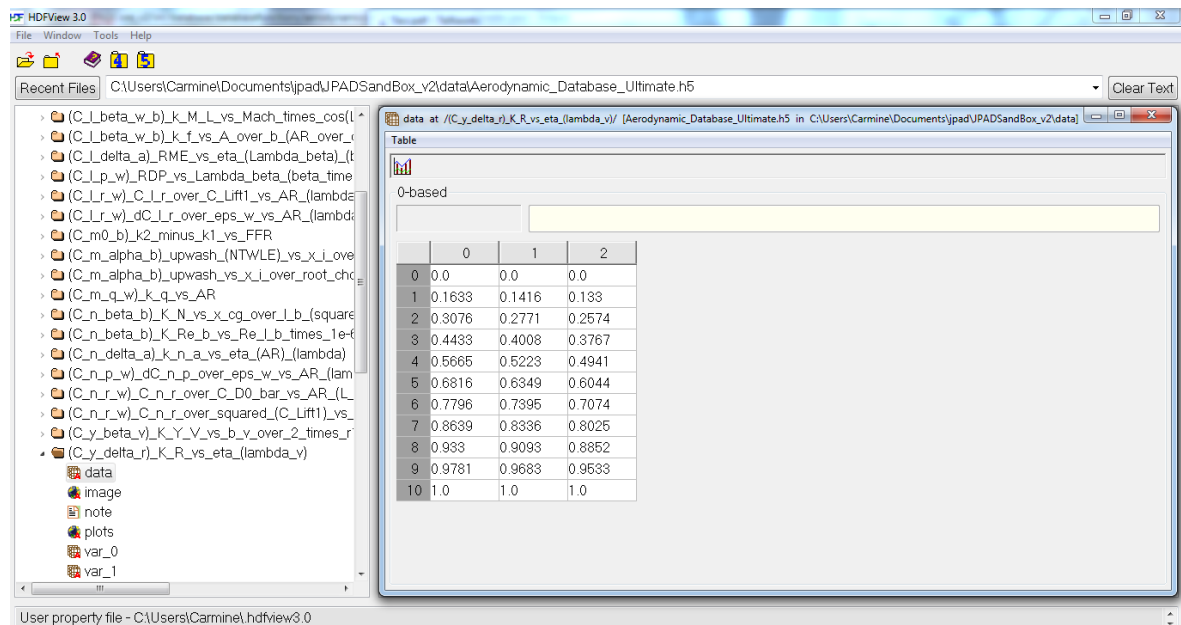


Figure A.3. Chart digitization using Grabbit

Listing A.2. Java extract from database reader class

```
public class AerodynamicDatabaseReader{

    private MyInterpolatingFunction C_y_delta_r_K_R_vs_eta_lambda_v;

    public AerodynamicDatabaseReader
    (String databaseFolderPath, String databaseFileName) {
        C_y_delta_r_K_R_vs_eta_lambda_v
        = database.interpolate2DFromDatasetFunction
        ("(C_y_delta_r)_K_R_vs_eta_(lambda_v)");
    }

    public double getCyDeltaRKRvsEtaLambdaV(
        double taperRatio,    // var0
        double eta            // var1
    ) {
        return C_y_delta_r_K_R_vs_eta_lambda_v.valueBilinear(
            eta,                // var1
            taperRatio          // var0
        );
    }
}
```

List of symbols

- $()_A$ quantity related to the ailerons.
- $()_B$ quantity related to the fuselage.
- $()_H$ quantity related to the horizontal tail.
- $()_R$ quantity related to the rudder.
- $()_V$ quantity related to the vertical tail.
- $()_W$ quantity related to the wing.
- $()_{WB}$ quantity related to the wing-fuselage configuration.
- \mathcal{AR} aspect ratio.
- b span.
- CG** Centre of Gravity.
- c chord.
- D aerodynamic drag.
- d maximum fuselage height at the wing-body intersection.
- L aerodynamic lift.
- \mathcal{L} aerodynamic rolling moment.
- l length.
- M Mach number.
- m mass.
- \mathcal{N} aerodynamic yawing moment.
- \bar{q} dynamic pressure.
- Re Reynolds number.
- S surface.
- SSM** static stability margin.
- W weight.

Y aerodynamic lateral force.

α_B angle of attack.

β sideslip angle.

Γ dihedral angle.

ε twist tip angle.

Λ sweep.

λ taper ratio.

Bibliography

- [1] Various Authors. *Grabit description*. URL: <https://www.mathworks.com/matlabcentral/fileexchange/7173-grabit>.
- [2] Various Authors. *Java (programming language)*. 2016. URL: [https://en.wikipedia.org/wiki/Java_\(programming_language\)](https://en.wikipedia.org/wiki/Java_(programming_language)).
- [3] DAR Corporation. *Advanced Aircraft Analysis*. 2017. URL: <http://www.darcorp.com/Software/AAA>.
- [4] A. De Marco et al. *A Java Toolchain of Programs for Aircraft Design*. Bucurest, Romania: CEAS, 2017.
- [5] J. Gosling et al. *The Java Language Specification*. 2015.
- [6] Hdf Groups. *HDF View Description*. URL: <https://support.hdfgroup.org/products/java/hdfview/>.
- [7] D. E. Hoak. *The USAF Stability and Control DATCOM*. Air Force Wright Aeronautical Laboratories, 1960.
- [8] Lissys Ltd. *Piano 5 for Windows*. 2017. URL: <http://www.piano.aero>.
- [9] M. R. Napolitano. *Aircraft Dynamics: From Modeling to Simulation*. John Wiley, 2012.
- [10] Oracle. *1.2 Design Goals of the Java Programming Language*. 2013.
- [11] D. Raymer. *RDS*. 2017. URL: <http://www.aircraftdesign.com/rds.shtml>.

